

Working paper

Climate Change, Aridity, and Internal Migration: Evidence from Census Microdata for 72 Countries

Roman Hoffmann, hoffmannr@iiasa.ac.at

Guy Abel, guy.abel@shu.edu.cn

Maurizio Malpede, maurizio.malpede@univr.it

Raya Muttarak, raya.muttarak@unibo.it

Marco Percoco, marco.percoco@unibocconi.it

WP-23-008

Approved by:

Name: Anne Goujon

Program: Population and Just Societies Program

Date: 24 July 2023

Table of contents

Abstract.....	3
About the authors	4
Acknowledgments	4
Introduction.....	5
Data and Methods.....	7
Data	7
Estimating global internal migration flows	9
Drought and aridity indicators	12
Standardization and rescaling of climate indicators	12
Statistical modeling.....	13
Predictions	15
Limitations	15
Results	17
Internal migration worldwide.....	17
Drought and aridity drive regional out-migration	18
Effects differ by world region and ecological zones	20
Migration impacts are moderated by contextual characteristics.....	22
Migration responses differ for different population groups.....	24
Discussion and conclusion	26
References	28
Supplementary Materials	33
Extended descriptive statistics	33
Further results and extended analyses	41

Abstract

Whether and to what extent climatic factors influence migration has received widespread public and scientific attention. In this paper, we focus on the impacts of increased aridity and drought on internal migration using novel census-based data for 72 countries covering the period 1960-2016. Analyzing information on 107,916 interregional migration flows, we find that drought and aridity have a significant impact on human mobility, particularly in the hyper-arid and arid areas of Southern Europe, the Middle East and North Africa, and Southern Asia. Migration is shaped by the level of wealth, agricultural dependency, and urbanization in the area of origin. Different age and education groups respond differently to droughts and aridity highlighting the importance of differential mobility patterns across population groups in different geographic contexts.

ZVR

524808900

Disclaimer, funding acknowledgment, and copyright information:

IIASA Working Papers report on research carried out at IIASA and have received only limited review. Views or opinions expressed herein do not necessarily represent those of the institute, its National Member Organizations, or other organizations supporting the work.

The authors gratefully acknowledge funding from IIASA and the National Member Organizations that support the institute (The Austrian Academy of Sciences; The Brazilian Federal Agency for Support and Evaluation of Graduate Education (CAPES); The National Natural Science Foundation of China (NSFC); The Academy of Scientific Research and Technology (ASRT), Egypt; The Finnish Committee for IIASA; The Association for the Advancement of IIASA, Germany; The Technology Information, Forecasting and Assessment Council (TIFAC), India; The Indonesian National Committee for IIASA; The Iran National Science Foundation (INSF); The Israel Committee for IIASA; The Japan Committee for IIASA; The National Research Foundation of Korea (NRF); The Mexican National Committee for IIASA; The Research Council of Norway (RCN); The Russian Academy of Sciences (RAS); Ministry of Education, Science, Research and Sport, Slovakia; The National Research Foundation (NRF), South Africa; The Swedish Research Council for Environment, Agricultural Sciences and Spatial Planning (FORMAS); The Ukrainian Academy of Sciences; The Research Councils of the UK; The National Academy of Sciences (NAS), USA; The Vietnam Academy of Science and Technology (VAST). The authors further acknowledge funding from the EPICCC (East Africa Peru India Climate Capacities) project which is part of the International Climate Initiative (IKI), the European Union (ERC consolidator grant, Population Dynamics under Global Climate Change (POPCLIMA), project number: 101002973), the Fondazione Invernizzi, and the National Science Foundation of China, General Program (Project number: 41871142).



This work is licensed under a [Creative Commons Attribution-NonCommercial 4.0 International License](https://creativecommons.org/licenses/by-nc/4.0/).

For any commercial use please contact permissions@iiasa.ac.at

About the authors

Roman Hoffmann is the Research Group Leader of the Migration and Sustainable Development Research Group (MIG) in the Population and Just Societies (POPJUS) Program at IIASA (Contact: hoffmannr@iiasa.ac.at).

Guy Abel is Professor in the School of Sociology and Political Science at Shanghai University and Researcher at the Asian Demographic Research Institute and in the POPJUS Program at IIASA (Contact: guy.abel@shu.edu.cn).

Maurizio Malpede is Assistant Professor of Economics at the University of Verona and Research Fellow at the GREEN Research Centre at Bocconi University (Contact: maurizio.malpede@univr.it).

Raya Muttarak is Professor of Demography at the Department of Statistical Sciences of the University of Bologna and Principal Research Scholar in the POPJUS Program at IIASA (Contact: raya.muttarak@unibo.it).

Marco Percoco is Associate Professor in the Department of Social and Political Sciences and Director of the GREEN Research Centre at Bocconi University (Contact: marco.percoco@unibocconi.it).

Acknowledgments

The Authors are grateful to Wendy Vanesa Ramírez González for valuable research assistance. R.H., G.A., and R.M. gratefully acknowledge funding from IIASA and the National Member Organizations that support the institute. R.H. acknowledges funding from the EPICC (East Africa Peru India Climate Capacities) project which is part of the International Climate Initiative (IKI). The German Federal Ministry for the Environment, Nature Conservation and Nuclear Safety (BMU) supports this initiative on the basis of a decision adopted by the German parliament. RM received funding by the European Union (ERC consolidator grant, Population Dynamics under Global Climate Change (POPCLIMA), project number: 101002973). MM and MP further acknowledge funding by the Fondazione Invernizzi, and GA by the National Science Foundation of China, General Program (project number: 41871142).

Introduction

Due to rising temperatures and changing precipitation patterns, many parts of the world are experiencing protracted drought and aridification trends. Drylands cover over 40% of the world's land area and are inhabited by approximately 2.5 billion people, or about one-third of the world's population (Burrell et al., 2020; FAO, 2019). By the end of the century, they are projected to increase by 11% under a medium Representative Concentration Pathway (RCP 4.5) and by up to 23% under a high (RCP 8.5) greenhouse gas emission scenario compared with the 1961–1990 baseline (European Commission/Joint Research Centre, 2018; Huang et al., 2016).

Changing climatic conditions and anomalies can particularly affect the livelihoods of people living in rural and agriculturally dependent areas and pose threats to food security, water availability, and health (Pörtner et al., 2022). When other adaptation options become limited, households may choose or be forced to migrate in response to increasing livelihood insecurity (McLeman and Smit 2006; Hunter, Luna, and Norton 2015). While in the public discourse, climate change is often portrayed as a cause of major international migration flows, numerous empirical studies and meta-analyses have demonstrated a more significant impact of environmental hazards and changes on short-distance, internal as opposed to cross-border mobility (Beine & Jeusette, 2019; Borderon et al., 2019; Cattaneo et al., 2019; Hoffmann et al., 2020; Šedová et al., 2021). Local economic, socio-political, and demographic conditions are essential in shaping migration patterns and outcomes (Black et al., 2011b).

However, due to data limitations, there is limited comparative evidence on the impact of gradual changes in climatic conditions on internal migration and the moderating role of contextual influences. Most evidence to date relies on country-specific case studies (Bohra-Mishra et al., 2017; Gray & Mueller, 2012; Mueller et al., 2014) and, in the case of cross-national analyses, proxy measures of migration, such as cross-country urbanization trends or population density estimates (Henderson et al., 2017; Marchiori et al., 2017; Niva et al., 2021). The World Bank's recent Groundswell Report, for example, uses a scenario-based approach that approximates the number of internal migrants in the future. It predicts that 216 million people globally may move within their countries' borders due to climate change by 2050 (Clement et al., 2021)

Here, we examine the impact of drought and aridification on global internal migration flows using a novel census-based internal migration dataset. The migration data are derived from census microdata provided by the Integrated Public Use Microdata Series (IPUMS) International for the period 1960–2016 (Minnesota Population Center, 2020). Using data from 201 censuses and 72 countries, we created a unique longitudinal database at the sub-national regional level (first-level administrative regions). Internal migration is estimated based on information on the census takers' previous and current region of residence one or five years prior to the census date. This allows us to calculate migration flows between each pair of regions in each country. The final dataset is composed of 1,410 census regions with 107,916 bilateral migration flows (Abel et al., 2022; Abel & Sander, 2014; Garcia et al., 2015).

To comprehensively model drought and aridity impacts, we use a range of composite indicators derived from different data sources (Beguería et al., 2010; Harris et al., 2020). We employ the UNEP Aridity Index (AI), the Palmer Drought Severity Index (PDSI), and the Standardized Precipitation Index measured over a three-month (SPEI03) and 12-month time frame (SPEI48). Whereas the first two measures are well-suited to capture long-

term aridification processes, the SPEI can also reflect shorter-term extreme events. Gravity-type fixed effects models are employed to estimate migration impacts across regions over time (26).

The harmonized data allow for a comprehensive analysis of the relationships between climatic change and inter-regional migration within a country across different geographical contexts. Although IPUMS also provides information on international migration, it does not specify the specific subnational origin regions of cross-border migrants. As this makes it more difficult to determine whether an international migrant was exposed to an environmental impact or not, we focus our analysis entirely on internal mobility. While previous studies have analyzed internal migration using IPUMS census data (Bell et al., 2015; Cirillo et al., 2022; Garcia et al., 2015; Lerch, 2020; Thiede et al., 2022), to our knowledge, this is the first large-scale longitudinal study of climate-induced internal migration that spans across all world regions.

Data and Methods

Data

Information on migration and socioeconomic conditions were derived from harmonized census microdata samples from the Integrated Public Use Microdata Series (IPUMS) International database (Minnesota Population Center, 2020). Each set of census microdata contains a small random sample (0.4%-10%) of unidentified private households and associated persons based on a full census conducted by the national statistical agency in each country. Countries used in the study were selected based on the availability of information on migration. In addition, we retrieved additional variables from the censuses on census takers' age, sex, education, and occupational profile.

The data were drawn from 201 different censuses covering the period 1960-2016 (Figure 1). While for some countries, data are available for up to 8 censuses (e.g., Mexico from 1960 to 2015), most countries have fewer observations over time, resulting in an unbalanced time series. In our estimation, we control for this by including decadal fixed effects in our estimation to rule out any confounding influences of the timing of the censuses.

The census data were combined with gridded time series data from the Climatic Research Unit (CRU) of the University of East Anglia (CRU TS, Version 4.07). The CRU TS dataset uses a 0.5° latitude by 0.5° longitude grid covering all land areas of the world, excluding Antarctica (Harris et al., 2020). The data provide monthly information from 1901 until 2022 on various climatic indicators, including temperature, precipitation, and potential evapotranspiration. The measures are based on interpolations (angular-distance weighting) of climate anomalies from an extensive network of weather stations worldwide.

In addition, information on drought conditions were retrieved from the SPEI database (SPEIbase v2.8: 1), which spans the period between January 1901 to December 2020 (Beguería et al., 2010). The SPEI calculations use the CRU monthly precipitation and potential evapotranspiration data employing the FAO-56 Penman-Monteith estimation for potential evapotranspiration. Like the CRU data, the SPEI database operates at a spatial resolution of 0.5 degrees and a monthly time resolution. It provides information on a range of SPEI timescales spanning from 1 to 48 months.

Finally, data were retrieved from the gridded global dataset for the Gross Domestic Product and Human Development Index spanning the period of 1990–2015 (Kummu et al., 2018). The database provides details about economic prosperity and human development with a resolution of five arcminutes, using various subnational sources. Consistency across time and space is ensured by calibrating the gridded estimates with reported national values, thereby maintaining representativeness at the national level.

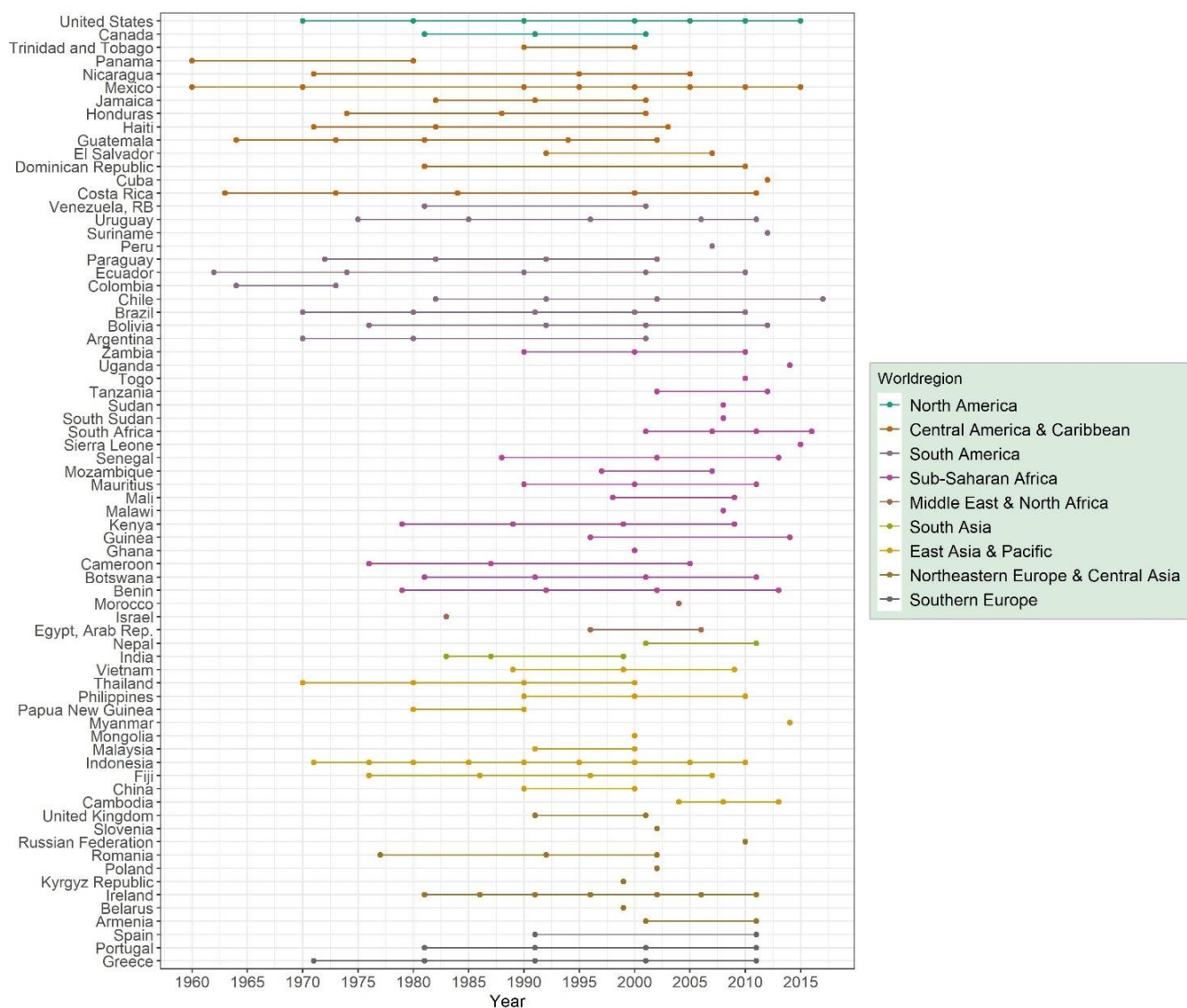


Figure 1. Timing of censuses across countries and world regions covered in the migration dataset.

The unbalanced longitudinal data contain information from 1960 to 2016.

Information from the gridded data products was extracted to the subnational regional level using harmonized first-level administrative regions shapefiles provided by IPUMS. The subnational units were harmonized so that their boundaries remain geographically stable over time. To account for changes in administrative boundaries over time, affected geographic units were merged to form larger and temporally stable units comprising two or more states, provinces, and similar entities. While most boundary changes involve the division of larger units into smaller ones, there are also instances where state or province boundaries have shifted. All variables in IPUMS align with the corresponding harmonized first-level geography codes, including variables referring to migration, allowing us to estimate migration flows between harmonized regions of origin and destination.

Estimating global internal migration flows

The migration measure used in our analysis is based on the census question about the census taker's previous subnational region of residence one or five years prior to the census and their current place of residence. For both questions, information on the first-level administrative region is provided in the data. This enables us to calculate the total flows of migrants between subnational regions of origin and destination in each country.

The question on the previous place of residence is asked differently in each country using a different temporal resolution, either (1) one year ago, (2) five years ago, or (3) length of stay in the current location. For the latter, where the continuous temporal period of stay is available, we reduced the information to a binary measure indicating whether or not the respondent has migrated in the past five years as a benchmark value. In total, 21.0% of all internal migration flows refer to migration within the past year and 79.0% to migration in the past five years.

Based on the information on the current and previous regions of residence, we calculate bilateral migration flows between region i and region j and vice versa in the past one or five years. The harmonized first-level administrative regions represent the units of analysis in our study. In total, we derived information on 107,916 bilateral migration flows covering a sample of 1,410 subnational regions. From the bilateral migration flows F_{ijt} , we derive an estimate of the annual migration rate M_{ijt} by dividing the flow measure by the total population P of region i at time t and by (2) the time interval I_{it} of one or five years considered for the migration measurement in the respective census:

$$M_{ijt} = \frac{F_{ijt}}{P_{it} \cdot I_{it}} \quad (1)$$

The constructed annual migration is typically lower for censuses that capture migration over a five-year instead of a one-year period. This is because circular migration patterns within that time frame are not recorded. To account for this, we control for the migration window considered in each census. Since the time intervals usually do not change between censuses, the differences should not largely affect our estimation of migration between subnational regions over time.

The map in Figure 2 shows the 72 countries included in this study: 2 countries from North America, 12 from Central America and the Caribbean, 11 from South America, 3 from Southern Europe, 9 from Northeastern Europe and Central Asia, 3 from the Middle East & North Africa (MENA), 19 from sub-Saharan Africa, 2 from South Asia, and 11 from East Asia and the Pacific. The inlay in the figure illustrates four exemplary migration flows between four regions in China. In Figure 3, we present actual migration data for six countries during the most recent census period. Circular migration plots (also known as chord diagrams) are used to visually represent the total number of migrants between different regions in each country.

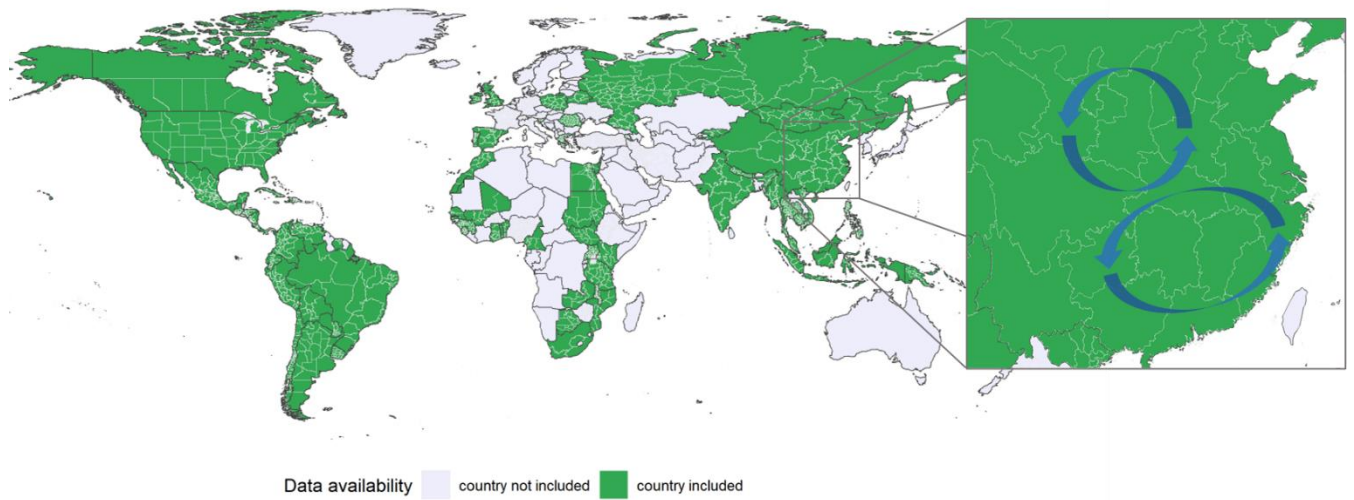


Figure 2. Countries and subnational regions included in the census migration database.

The map shows the boundaries of the subnational regions, which form the basis of the migration flow estimation. The inlay to the right shows exemplary migration flows between four regions in China.

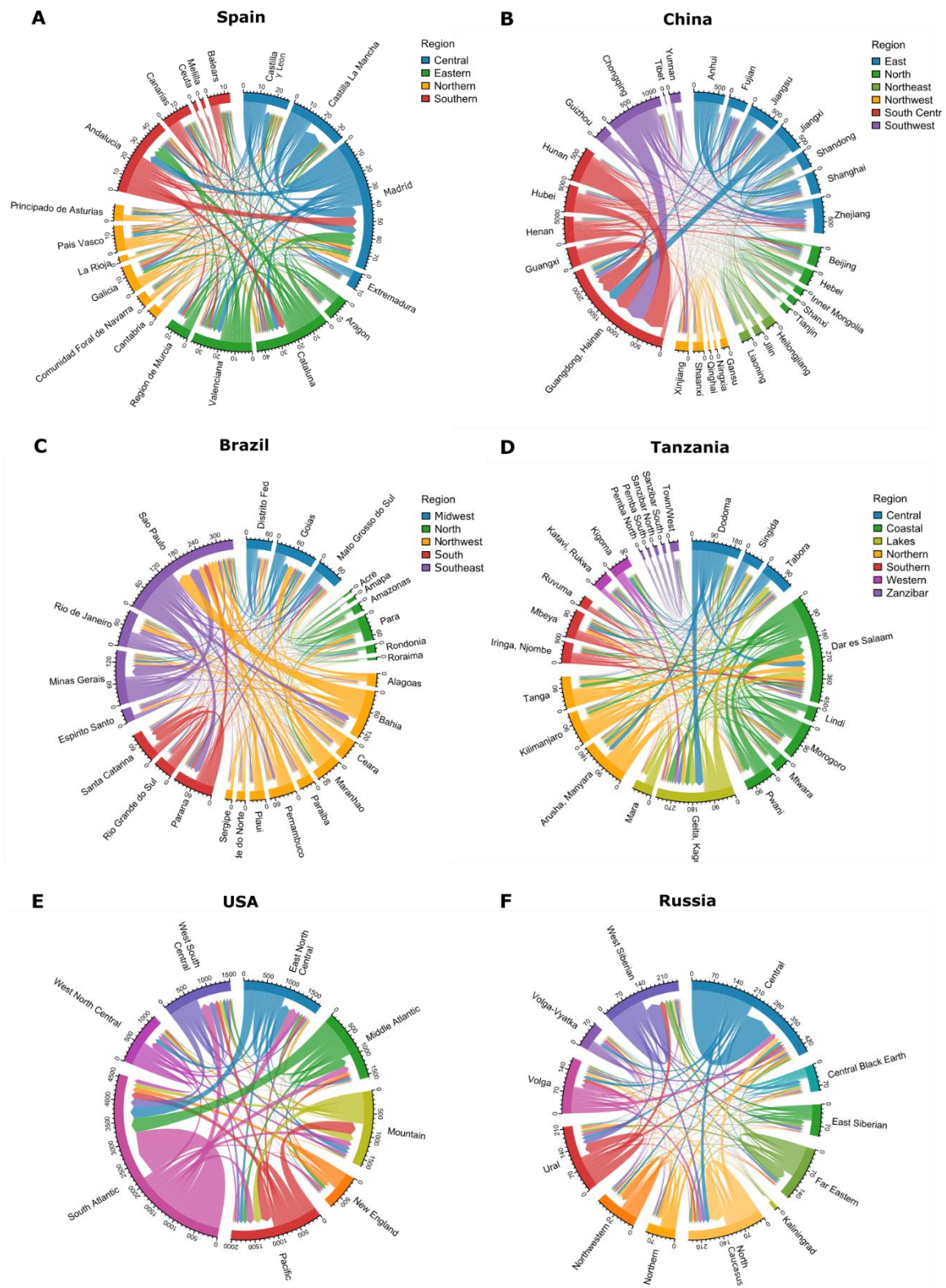


Figure 3. Circular migration plots showing migration flows between subnational regions in exemplary countries.

The migration flows were estimated using the latest available census. Panels A Spain, B China, C Brazil, D Tanzania, E USA, F Russia. Subnational regions in the USA and Russia were further aggregated due to the large number of regions.

Drought and aridity indicators

Based on the derived climate data, we prepare four key indicators to measure changes in aridity and drought in the subnational regions over time.

(1) The aridity index (AI) measures dryness as the ratio between the yearly precipitation and potential evapotranspiration (PET) in an area. Lower values of the AI represent higher dryness, with areas with an AI below 0.05 being classified as hyper-arid, below 0.20 as arid, below 0.5 as semi-arid, below 0.65 as dry subhumid, and above 0.65 as humid. The AI is particularly suitable to reflect longer-term changes in aridity and persistent drought conditions.

(2) As a second measure of dryness, we consider the Palmer Drought Severity Index (PDSI), which is based on temperature and precipitation data to assess relative dryness. This standardized index typically ranges from -10 (dry) to +10 (wet), although more extreme values are possible. Like the AI, the PDSI is used to quantify long-term drought and aridity by considering potential evapotranspiration through temperature data and a water balance model. However, it has limitations in detecting droughts on time scales shorter than 12 months. It also lacks multi-timescale features found in other indices like SPI and SPEI, making it difficult to correlate with specific water resources such as runoff, snowpack, and reservoir storage. In our analysis, we use the self-calibrating version of the PDSI, which helps to address comparability issues across different regions.

(3) For the final two climate indicators, our analyses use the Standardized Precipitation Evapotranspiration Index (SPEI). The SPEI measures the water balance in a region based on both the local precipitation and potential evapotranspiration. The SPEI measure is particularly useful for detecting drought events over a shorter or medium time period. The SPEI is centered around the value of zero, with positive values indicating higher humidity and negative values drier conditions. Areas with a SPEI below -1.5 are considered severely dry, and areas with a value below -2.0 extremely dry. Here, we use two SPEI-based variables, one which considers the water balance accumulated over a rolling 3-month period and one over a longer 12-month period, allowing us to capture water imbalances and drought conditions over shorter periods to complement the other climatic indicators.

For sensitivity analyses, we use the Normalized Difference Vegetation Index (NDVI) as an additional indicator. The NDVI is a remote sensing measure showing the amount of green vegetation and can thus serve as a proxy for dryness in an area. By design, it is limited to values between -1.0 and +1.0, with lower values indicating drier conditions. The indicator is available from 1981 and hence covers a shorter time period compared to the other indicators, which are available from 1901. All aridity indicators are similarly scaled, with smaller values indicating drier and larger values indicating more humid conditions. For our analysis, the indicators were rescaled so that larger values indicate greater dryness.

Standardization and rescaling of climate indicators

The use of complementary climatic indicators allows us to comprehensively explore drought and aridity impacts over longer and shorter periods. To allow for comparisons across the different measures, all indicators were standardized. For this, we use the information on the measures' distribution across different geographical scales.

For the main models, all indicators were standardized at the subnational regional level. For this, the long-run regional mean of the drought and aridity variables \bar{C}_i in a region i was subtracted from the observed annual values C_{it} and divided by the long-run standard deviation $\sigma(C)_i$ of the variable. The resulting standardized anomaly measures $C_{stan,it}$ show the standardized deviation in drought conditions and aridity in a region from the long-run normal conditions in a reference period:

$$C_{stan,it} = \frac{C_{it} - \bar{C}_i}{\sigma_{C_i}} \quad (2)$$

Here, we consider as reference the period from 1901 to 2016 for the calculation of the long-run mean and standard deviation. All results are robust to using shorter reference periods (1960-2016) and to using a rolling reference period window (50 years prior to each census date), allowing to account for adaptation effects (Dell et al., 2014; Hsiang, 2016). For additional robustness tests, we used the unstandardized climatic indicators and indicators using the country-wide distribution or the global distribution of the variables as the basis for the standardization.

The original versions of the drought and aridity variables considered are scaled so that negative values indicate drier and positive values more humid conditions. To facilitate the interpretation of the results, we rescaled the variables so that positive values indicate greater dryness and negative values more humid conditions. Accordingly, positive model coefficients refer to a positive effect of drought and greater aridity on migration, and negative coefficients to a negative effect, making the interpretation more intuitive for readers. The findings show the effect of a one standard deviation increase in dryness for the respective indicators on migration.

Statistical modeling

The impacts of climatic changes and hazards on migration are estimated using a series of fixed effects panel models, which regress the bilateral out-migration rate between regions of origin i and destination j on the different aridity and drought indicators $C_{stan,it}$. Our models are estimated parsimoniously to avoid overcontrolling issues (Hsiang, 2016). All models control for the respective time interval (five vs. one year) used for measuring migration flows between the region of origin and destination. The full model can be written as:

$$\ln(M_{ijt}) = \beta C_{stan,it} + I_{it}\gamma + \log(D_{ij})\delta + A_{ij}\rho + \alpha_i + \delta_j + W_r\theta_t + \varepsilon_{ij,t} \quad (3)$$

Where M_{ijt} is the annual out-migration rate from a region i to a region j at time t . $C_{stan,it}$ refers to the vector of climate indicators in the origin region (Beine & Parsons, 2015). In further models, we extend this baseline specification by simultaneously considering changes in environmental conditions in the destination areas $C_{stan,jt}$ (Supplementary Table S16). I_{it} captures the migration time interval (one vs. five years) considered in the census.

Unobserved spatial heterogeneity is controlled for via the use of region of origin (α_i) and destination (δ_j) fixed effects. These account for relatively stable characteristics of the regions over time, including cultural differences,

political systems, and climatic zones, which could otherwise confound the estimation. For the estimation, we follow a gravity-type modeling approach, controlling for the logged distance D_{ij} between origin and destination as well as an indicator variable A_{ij} that measures whether origin and destination regions are adjacent to each other (Beine et al., 2016; Beine & Parsons, 2015).

To account for confounding influences of temporal trends, we control for world region-specific time trends through the use of time-fixed effects ($W_r\theta_t$). The time-fixed effects are estimated using decadal period dummies, which we interact with world region dummies to capture differing time trends in each macro-region in our data. The results are fully robust when controlling for time-fixed effects in the form of five-year time steps and estimating country-specific trends. $\varepsilon_{ij,t}$ is the random error term capturing the remaining unexplained variation in the data. To estimate robust standard errors, all standard errors were clustered at the level of the origin region.

In our baseline specification, the climatic indicators are aggregated over a period of ten years prior to the census date to capture broader changes in environmental conditions. This time window reflects the typical period between two censuses. The results are robust to the use of shorter time windows of five years. We also find consistent results for changes in the AI and PDSI for longer time windows of 20 years, but the SPEI coefficients are no longer significant. The SPEI measures are especially suitable for capturing shorter-term drought events whose influences may vanish when considering longer time periods.

Equation (3) is estimated using the Poisson-pseudo maximum likelihood (PPML) estimator, which accounts for the right-skewness and zero inflation of the migration outcome (Santos Silva & Tenreyro, 2006). The estimator also allows for unbiased estimates if any of the covariates of Equation (3) are correlated with higher moments of the error term, which can be a problem in log-linear models (Beine et al., 2016). The estimation is implemented in R using the *fixest* package (Bergé, 2018). As we control for origin and destination fixed effects, the models build on variation within regions over time. Since changes in environmental conditions over time are plausibly exogenous conditional on geographic location and time trends, our model allows estimating the causal impacts of changes in drought and aridity on migration.

We use interaction models to explore differential climatic impacts by ecological and socioeconomic characteristics of regions of origin and destination. A particular advantage of our census-based data is that they do not only allow us to estimate the extent of the migration flows but also to explore who was migrating based on the migrants' characteristics and where they moved to, based on information about the destination regions. For this, we further distinguish migration flows by underlying demographic characteristics of the census respondents, distinguishing between the migration of people with different educational backgrounds (no education, primary, secondary, or tertiary) and age groups (0-14, 15-20, 21-25, 26-30, 31-45, 46-60, >60) by sex (male, female). Due to the small size of specific demographic groups in some regions, the estimation of accurate migration flows is more challenging. To account for this, outliers with a migration rate larger than 10% were removed from the subgroup analysis (<1% of observations).

Predictions

Based on the empirical findings, we provide explorative predictions of potential migration changes under a 4°C global warming scenario. For this prediction exercise, we combine (1) the results from statistical models estimating differential migration responses to changes in the aridity index by world regions and baseline levels of aridity (Supplementary Table S8) with (2) data on projected changes in the aridity index until the end of the century (Supplementary Figure S5).

To define the baseline aridity level, we consider the mean aridity index in the origin regions in the reference period 2001-2020. Based on this average, we classify regions into hyper-arid/arid ($AI < 0.2$), semi-arid/sub-humid ($0.2 \leq AI < 0.65$), and humid regions ($AI \geq 0.65$) and estimate whether changes in drought and aridity over time are more impactful in regions characterized by an overall drier climate. Based on the significant estimates, we derive predicted marginal effects for each world region and aridity level.

We combine these effects with gridded projection data on expected changes in the aridity index by the end of the century provided by Wang et al. (2021). The projections are based on outputs from 21 Coupled Model Intercomparison Project Phase 5 models under the Representative Concentration Pathways 8.5 (RCP8.5) scenario. They project changes in the aridity index at 2°C and 4°C levels of global warming. According to the projections, more substantial increases in aridity are expected in the northern high latitudes. An expansion of drylands is expected in both semi-arid and arid regions.

Limitations

The employed migration data and empirical strategy come with certain limitations which are important for the interpretation of the results reported in this study. While the harmonized census migration data provide a unique dataset to comprehensively analyze internal migration worldwide, the derived information is available only at a coarse temporal and spatial scale.

Given that censuses are collected only every decade for most countries, shorter-term changes in mobility are difficult to capture. Also, most censuses employ a broad time window of five years when asking census takers about their previous place of residence. While this enables us to capture mobility over longer time horizons, we may miss migration over shorter periods and more circular forms of mobility. At the time of the census, some people may have already migrated back to their origin regions or moved on to another region in the country. Also, more seasonal forms of mobility are not captured in our migration measures.

Although we can use migration data to estimate the movement of people between regions, we cannot capture mobility at a more granular level within subnational regions. As most climate-related mobility occurs within shorter distances (Hunter et al., 2015), our models will likely produce conservative estimates of drought and aridity impacts on migration. Also, due to differences in the size of administrative units across countries, short-distance mobility may be better reflected in some areas than others. While this would not affect our model estimates, which are entirely based on within regional changes over time, it can be relevant for the external validity of our findings for different world regions. Also, due to the unbalanced migration time series, our estimates rely more on countries with more observations over time.

While the migration data considered in this study comprehensively map internal migration flows, international migration is not captured. Although IPUMS census data can provide information on international mobility, it only includes the previous country of residence of the census-taker without specifying the subnational regions of origin within that country from where the international migrant came. As our models rely on regional changes in climatic conditions, an estimation of drought and aridity impacts on international migration was not possible. As most climate-related mobility occurs within country borders, international migration flows are expected to be less relevant in the context of our study (Hoffmann et al., 2020; Hunter et al., 2015).

The harmonized migration data provide a unique database for understanding internal mobility and comparing climatic impacts across different contexts and for different subgroups in the population. Due to the high context-sensitivity of climate-related mobility, this data add essential insights into migration decision-making processes and the role of local conditions. Beyond studying environmental impacts on migration, the data offers other applications, including studying migration impacts of changes in local economic conditions and conflicts.

Results

Internal migration worldwide

Patterns of internal migration differ substantially across countries and sub-national regions. Considering areas with disproportionately high and low levels of annual out-migration relative to the country mean (Figure 4A), we observe high and low mobility clusters. Country-specific topographic and socio-economic characteristics are important for shaping migration patterns. For instance, in China, western regions are characterized by higher out-migration, whereas lower levels of out-migration and higher immigration are observed in eastern coastal regions where major economic activities concentrate. In Russia, on the other hand, out-migration is higher in the eastern parts of the country and lower in the more urbanized western parts. In the US, Canada, and Brazil, out-migration is highest in the central parts of the countries and in Argentina in the South.

In extended analyses (Supplementary Table S4), we test for the role of regional characteristics in shaping out-migration. We find that most migration is over short distances and between neighboring provinces. The bilateral migration rate is estimated to be 0.09 percentage points [CI90: 0.074,0.106] higher between adjacent as opposed to non-adjacent regions of a country. Regions at the periphery of a country with an international land border have an on average 0.03 percentage points [CI90: 0.014,0.046] higher out-migration rate as opposed to regions without a border.

Using census-based information on urban population shares in origin and destination regions, we find considerably higher migration to urban as opposed to rural areas, highlighting the importance of rural-urban moves for internal migration. Likewise higher out-migration is observed towards regions with a higher GDP per capita and a lower agricultural employment share. At the country level, regions in countries with higher income inequality exhibit higher out-migration rates on average.

Analyzing changes in migration flows between regions of origin and destination over time, we find increases in internal migration over the past decades, particularly after the 1980s (Figure 4B). In the 2000s, internal migration was estimated to be 50.5% [CI90: 45.8, 64.2], and in the 2010s, 79.3% [CI90: 66.3, 89.5] higher compared to the 1960s.

Utilizing the IPUMS census data enable us to further discern the migration patterns of distinct population subgroups, considering factors such as age, sex, and educational attainment. In line with the existing migration literature (Levy & Wadycki, 1974; Manning & Trimmer, 2020), we find distinct migration patterns by age (Figure 4C) and education (Figure 4D). Mobility is highest among individuals aged 15 to 30 as well as among the more educated. Better labor market prospects and increased mobility among young adults are likely explanations for this finding. Across various age and education groups, the mobility is found to be slightly higher for men compared to women (Abel & Cohen, 2022).

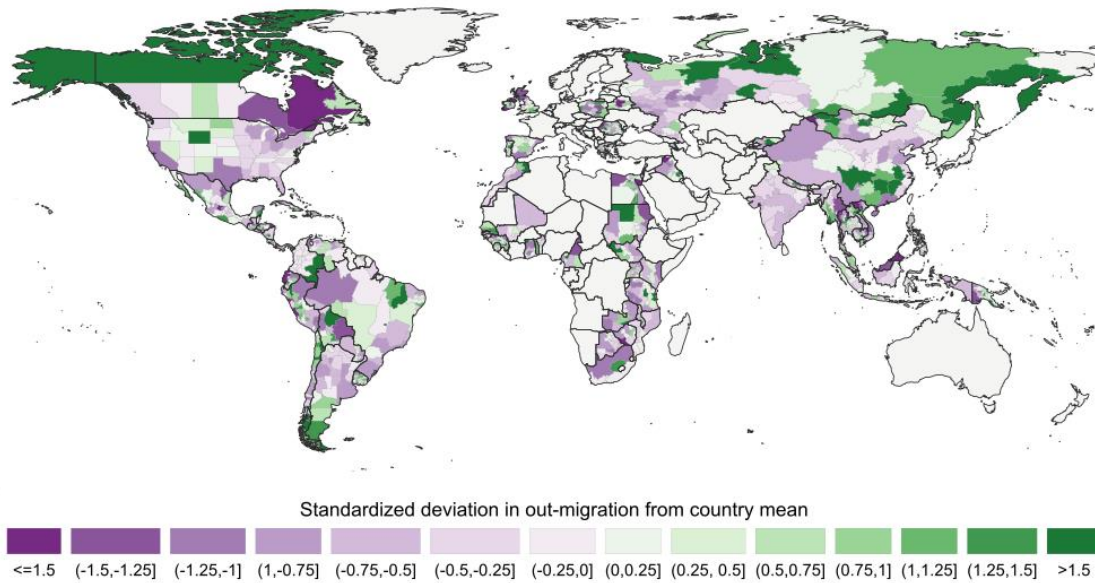
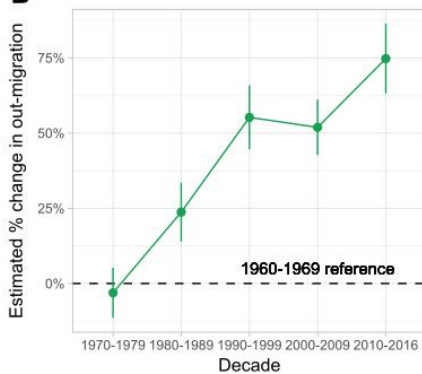
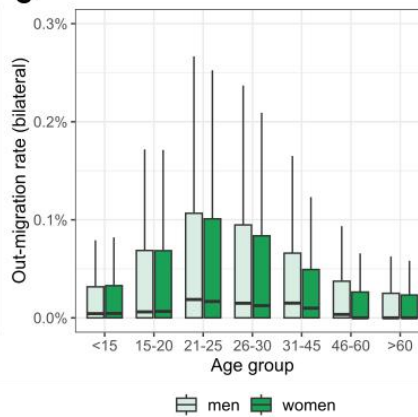
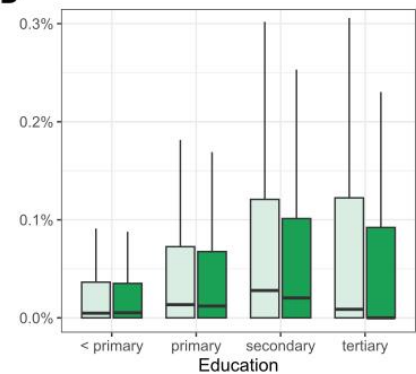
A**B****C****D**

Figure 4. Patterns in internal migration worldwide.

Panel A shows the standardized deviation of the regional out-migration rates from the country-specific mean for the last available census. The standardization ensures the comparability of the information across different country contexts and administrative settings. Regions with an above-average out-migration rate are shown in green, and regions with a below-average out-migration rate are shown in purple. Countries colored in grey are those not available in our database. Panel B shows the modeled temporal trends in internal migration worldwide using the period 1960-1969 as a reference (Supplementary Table S5). Panel C shows differences in regional out-migration rates by age and sex, and Panel D by education and sex. The boxplots show the median, interquartile ranges (IQR), and $1.5 \times$ IQR of the distributions across sub-national regions.

Drought and aridity drive regional out-migration

To test for the impacts of drought and aridity, we combine the sub-national bilateral migration data with information on climatic conditions in the regions of origin ten years prior to the census date. All drought and aridity measures were rescaled to facilitate interpretation, with positive values reflecting increased drought severity or dryness, respectively. Longitudinal models are used to identify the environmental impacts on internal migration (Table 1).

The models study changes in migration from one region to another and test whether these changes are affected by changes in the climatic conditions in the origin areas. All models control for region of origin and destination fixed effects and world region-specific time trends. We also performed several robustness and falsification tests to check for the sensitivity of the results. All results remain fully robust to variations in the model specification, weighting and standardization approaches, time windows considered, and the conceptualization of the migration and climate measures.

Table 1 – Baseline models estimating impacts of drought and aridity on out-migration rate

	Outcome: Annual out-migration rate				
	(1)	(2)	(3)	(4)	(5)
AI		0.0662*** (0.0199)			
PDSI			0.0492*** (0.0155)		
SPEI03				0.0722*** (0.0212)	
SPEI12					0.0583*** (0.0190)
Log(distance)	-0.7632*** (0.0407)	-0.7636*** (0.0407)	-0.7635*** (0.0407)	-0.7636*** (0.0407)	-0.7635*** (0.0407)
Adjacent regions	0.6325*** (0.0861)	0.6326*** (0.0861)	0.6324*** (0.0861)	0.6325*** (0.0862)	0.6325*** (0.0861)
Time window of 5 years	-0.1639 (0.1246)	-0.1575 (0.1252)	-0.1519 (0.1250)	-0.1335 (0.1269)	-0.1350 (0.1284)
World region x decade FE	Yes	Yes	Yes	Yes	Yes
Origin FE	Yes	Yes	Yes	Yes	Yes
Destination FE	Yes	Yes	Yes	Yes	Yes
S.E.: Clustered	by: origin	by: origin	by: origin	by: origin	by: origin
Observations	107,916	107,916	107,916	107,916	107,916
Pseudo R2	0.22845	0.22857	0.22849	0.22857	0.22854
BIC	34,224.90	34,236.30	34,201.60	34,236.30	34,236.40

Note: PPML fixed effects, gravity models. Poisson regression coefficients with cluster robust standard errors in parentheses. Clustering of standard errors at the origin region level. Input variables: Aridity Index (AI), Palmer Drought Severity Index (PDSI), Standardized Precipitation Evapotranspiration Index (SPEI). SPEI03 and SPEI12 refer to aggregated 3 and 12 months SPEI, respectively. All drought and aridity variables were rescaled so that larger values indicate more severe drought or greater dryness. The outcome variable is the annual out-migration rate. The variable distance refers to the Euclidian distance between the centers of two regions. The variable time window of 5 years indicates that the census used a five-year time window to capture migration. P-values: * 0.1 ** 0.05 *** 0.01

We find significant and sizeable effects of drought and aridity on migration. A one standard deviation change in the aridity index (model 1) is estimated to lead to a 6.62% (CI90: 3.36, 9.88) change in the annual out-migration rate in the affected region. Similar effect sizes are found for the PDSI (model 2), SPEI03 (model 3), and SPEI12 (model 4), which are estimated to lead to an increase in migration of 4.92% [CI90: 2.38,7.46], 7.22% [CI90: 3.74,10.70], and 5.83% [CI90 2.71,8.95], respectively, pointing to a high consistency in the effects of water stress and dryness on human mobility.

To ensure the validity of our empirical design, we conducted a placebo test analyzing the correlation between the out-migration rate and the lead values of the climate indicators in the period 10 years after the census (Supplementary Table S15). We do not find significant evidence that future drought or aridity predict past mobility suggesting that our empirical design is valid. In further models (Supplementary Table S16), we tested for the impacts of changes in the climatic conditions in the prospective destinations but did not detect any consistently significant results. This suggests that the conditions in the origin regions may be more relevant in influencing migration decisions.

We also analyzed non-linearities in drought and aridity impacts on migration (Supplementary Table S6). We find evidence that as environmental stress levels rise, the impact on migration increases. The dryer the conditions in an area, the more substantial the migration impacts. This finding may be due to nonlinearities in the migration responses (McLeman, 2018; Meze-Hausken, 2008; Nawrotzki et al., 2017). When faced with significant pressure, households may eventually reach a point where relocation becomes the only viable option, as coping and adapting may no longer be feasible (Dow et al., 2013; Hoffmann et al., 2022; Warner et al., 2012).

Effects differ by world region and ecological zones

Using a series of interaction models, we test for differences in migration impacts for different world regions (Figure 5), revealing significant geographical and contextual heterogeneity in migration responses. We find the most consistent and strongest impacts of all considered climate indicators on migration in Southern Europe, the Middle East and North Africa (MENA), and South Asia. A change in the aridity index by one standard deviation is estimated to increase out-migration by 58.7% [CI90: 48.3,69.0] in Southern Europe, by 30.2% [CI90: 7.7,52.6] in the MENA region, and by 41.9% [CI90: 41.9,50.8] in Southern Asia, respectively.

Positive but weaker effects are observed for countries in South America and sub-Saharan Africa, where changes in the aridity index are estimated to lead to a 11.4% [CI90 6.6,16.2] and 4.2 % [CI90 1.0,7.4] increase in migration, respectively. No significant impacts are observed in Northeastern Europe and Central Asia, East Asia and the Pacific, and North America. For Central America and the Caribbean, negative effects are estimated for all climatic indicators, suggesting that wetter periods potentially due to more extreme storms are related to higher out-migration from those areas. These results also depend on the subsets of countries available and should not be interpreted as a fully representative picture of a particular region.

In further extended analyses (Supplementary Table S8), we find heterogeneity in the magnitude of the effects across baseline levels of dryness in the origin region (reference period 2001-2020). The strongest migration responses are found in hyper-arid and arid regions, which are already characterized by high levels of dryness, high temperatures, and limited rainfall. Future increases in aridity may lead to desertification and land degradation in these areas contributing to lower crop productivity, putting further pressure on the livelihoods of the already vulnerable local populations (Dow et al., 2013; Warner et al., 2012).

We use the results of these extended models for explorative predictions combining the estimated differential migration responses by world region and baseline aridity level with projections of future changes in the aridity index at two and four degrees of global warming by the end of the century (Wang et al., 2021). The results

(Figure 5B) suggest large regional differences in the relevance of drought and aridity for human mobility. Particularly in dryland areas in the Mediterranean, South America, Central Asia, and North America migration patterns are expected to be affected by future drying trends.

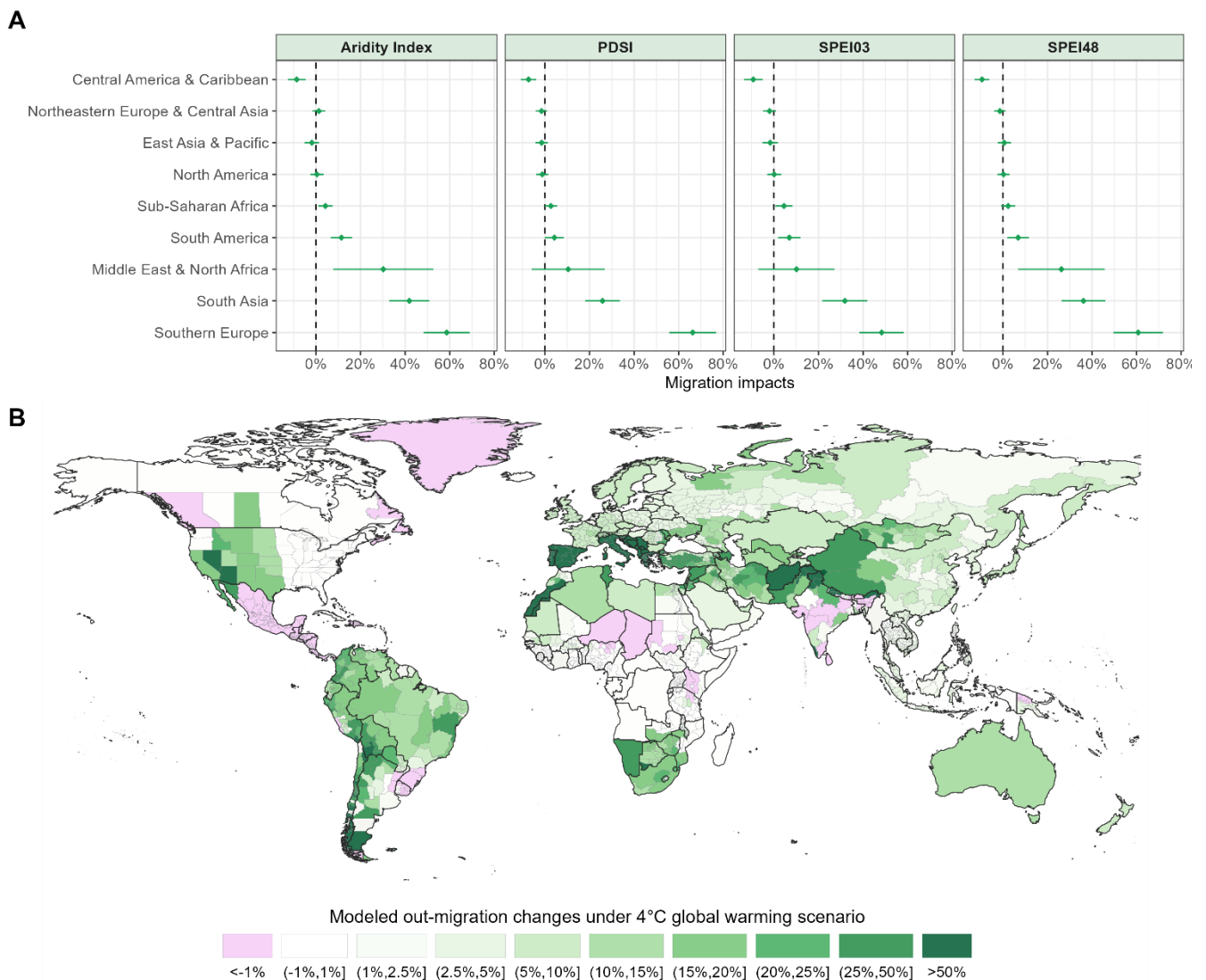


Figure 5. Differences in migration impacts of drought and aridity across world regions.

Panel A shows differences in migration impacts by the geographical location of the sub-national regions distinguishing effects across world regions. The x-axis shows the marginal effects and 90% confidence intervals of a one standard deviation increase in aridity levels on out-migration rates. The underlying full models are displayed in Supplementary Table S7. Panel B shows modeled migration changes under a 4°C global warming scenario based on projected changes in dryness in the regions until the end of the century (Wang et al., 2021). For the prediction, extended models (Supplementary Table S8) were used to estimate differential migration responses by world region and baseline aridity level (reference period 2001-2020) distinguishing between hyper-arid/arid, semi-arid/sub-humid, and humid regions. The derived predicted marginal effects were combined with the projected changes in the aridity index in the regions to explore potential impacts on internal migration.

Migration impacts are moderated by contextual characteristics

The substantial differences across regions suggest that local socio-economic and political conditions may play an important role in moderating the effects of increased drought and aridity on migration. Based on a number of extended models, Figure 6 shows changes in the estimated migration response (y-axis) by different interaction variables measuring local background characteristics at the regional level.

The graphs illustrate changes in the marginal effects of a one standard deviation increase in the four climate indicators. Panel A displays interactions with the GDP per capita, the agricultural employment share, and the urban population share in the origin regions. Panel B shows interactions with the standardized deviations of these measures from their country-specific means. The first set of measures reveals variations in migration responses according to the origin's socio-economic characteristics. The second set focuses on intra-country disparities. For the latter measures, we distinguish the influence of characteristics of origin (solid lines) and destination regions (dashed lines) in influencing migration impacts.

The regional income level, agricultural dependency, and level of urbanization influence interregional migration in response to environmental changes. Considering first the differences in the characteristics across all regions in the sample, we find overall stronger migration responses in wealthier regions, regions with a higher agricultural employment, and regions with a lower urban population share. The findings suggest that migration barriers or resource constraints hamper mobility attenuating the migration effects in poorer areas. Liquidity constraints could, for example, be exacerbated in the face of environmental stress, leading to the possibility of populations becoming "trapped" or "immobile" (Benveniste et al., 2022; Cundill et al., 2021; Farbotko et al., 2020; Mallick & Schanze, 2020; Nawrotzki & DeWaard, 2018; Zickgraf & Perrin, 2016).

The strong effects in rural and agriculturally dependent areas suggest that these areas are particularly vulnerable to drought and aridity due to their impacts on agricultural production and livelihoods. Especially in low-income countries, agriculture represents an important economic sector and provider of local food supplies (Mendelsohn, 2008; Schlenker & Lobell, 2010). Differential necessities to migrate in response to environmental stress can hence moderate the effects (Hoffmann et al., 2020). These results also hold when using country instead of region-level background characteristics (Supplementary Figure S6). Considering differences between countries, we also find reduced mobility responses the higher the inequality in a country.

When considering differences within countries, we find that migration flows from less urbanized to more urbanized regions to be more impacted by changes in drought and aridity. Additionally, our findings indicate that regions with a higher share of agricultural employment experience more out-migration (solid lines). However, no clear patterns are visible in terms of destination areas (dashed lines). The agricultural employment situation in destination areas does not appear to be a decisive factor in determining the migration destination choice of individuals affected by drought and aridity.

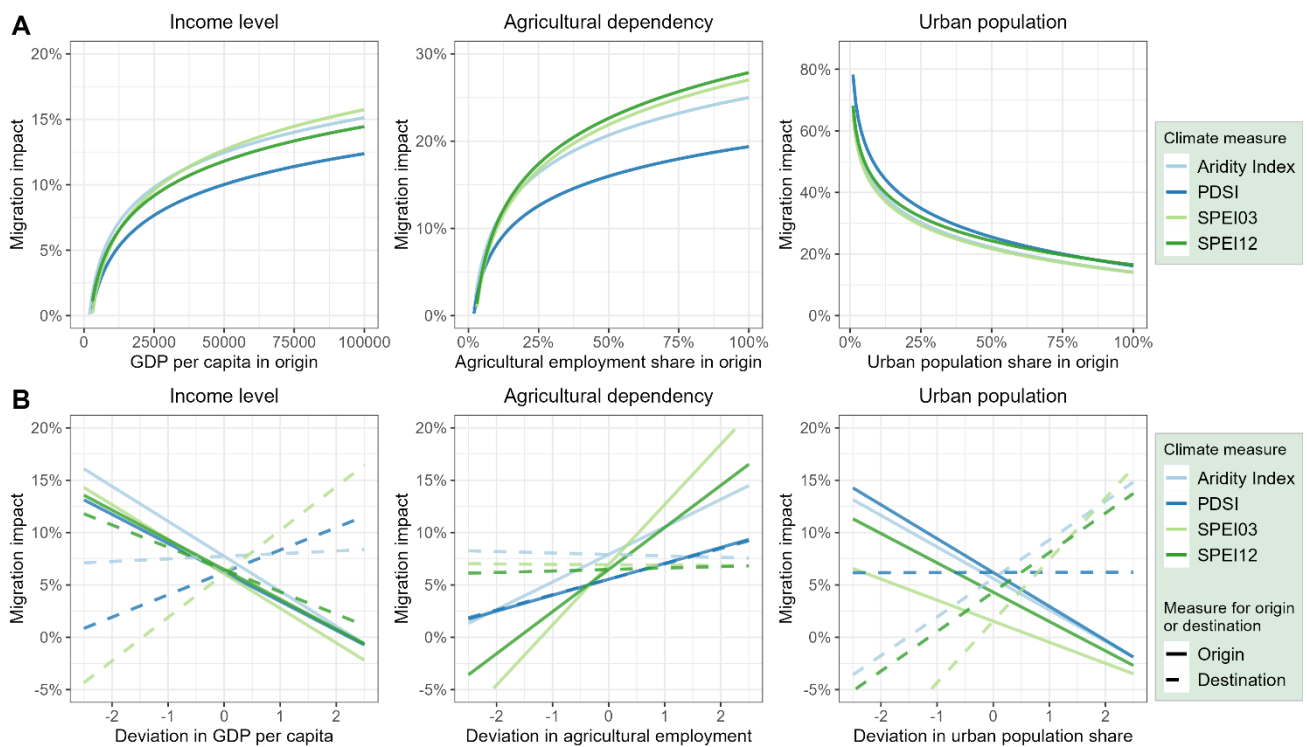


Figure 6. The role of regional background characteristics in shaping migration responses to drought and aridity.

Panel A illustrates the role of regional characteristics in influencing migration responses to drought and aridity. The y-axis shows the marginal effects of a one standard deviation change in the climate indicators on the out-migration rate. The figures rely on model estimates considering interactions between the climate indicators and the GDP per capita, the agricultural employment share, and the urban population share in the regions of origin (Supplementary Tables S9-S11). Increasing (decreasing) functions indicate increasing (decreasing) migration impacts with higher levels of the interaction variable. All models estimating interactions with agricultural employment and urban population share also control for interactions with GDP per capita to rule out confounding wealth effects. Panel B shows the results of interaction models interacting the climate indicators with regional deviations in GDP per capita, agricultural employment, and urban population share from the country-specific mean (Supplementary Tables S12-S14). Considering standardized deviations as opposed to the overall level values of the variables allows testing for differences in migration responses by within-country differences in wealth, agricultural dependency, and urban population. Solid lines show the results where interaction variables refer to deviations in origin areas. Dashed lines show the results for deviations in destination areas.

Although migration responses were overall stronger in richer regions, indicating that a certain level of wealth is necessary to enable mobility, the within-country analysis reveals a more nuanced pattern. Here, we find that regions with comparatively lower wealth in a country experience a higher rate of out-migration. A one standard deviation increase in within-country GDP, on the other hand, is associated with a 3.39% [CI90, -5.59, -1.19%] reduction in the migration impact of a one standard deviation increase in the aridity index. This suggests that while we see overall higher levels of mobility in wealthier countries, it is often the poorer regions within those countries where populations respond more strongly when exposed to drought or increased aridity. We find an inconsistent influence of the wealth levels in destination areas suggesting more mixed patterns when it comes to the role of destination area characteristics in shaping climate mobility.

Migration responses differ for different population groups

As a final step, we examine which population groups are most likely to migrate in response to increased aridity and drought. For this, we categorize the census participants into different subgroups and estimate group-specific migration flows from one region to another. We classify migration flows by sex, age groups (0-14, 15-20, 21-25, 26-30, 31-45, 46-60, >60), and education levels (less than primary, primary, secondary, or tertiary). Figure 7 shows marginal effect plots where the coefficient and confidence intervals are plotted (y-axis) for the different subgroups (x-axis). In the analysis, we further distinguish between less developed (top figures) and more developed (bottom figures) countries, two groups that reveal significant differences in age and education-specific migration responses.

Focusing on differences by age and sex (Figure 7A), we find highly consistent patterns across the different climate indicators. Overall, migration responses across age groups are more pronounced in more developed than in less developed contexts. While we find a hump-shaped distribution in less developed countries, with the middle age groups showing the strongest migration response, it is the older age groups in more developed countries who show the strongest response.

Whereas the pattern in lower-income contexts suggests a higher out-migration of the working-age population, we see an opposite effect in higher-income contexts, where older population groups are more mobile. This could be due to a generally higher mobility among older groups or retirement migration, where individuals move to areas with a more pleasant climate (Savaş et al., 2023). In less developed countries, men are more likely to migrate in response to environmental stress in some age groups (e.g., 26-30). However, the gender differences are not consistent across all age groups considered.

Also, for education (Figure 7B), differences in patterns are visible between less and more developed countries in the sample. Our results indicate a positive education gradient in less developed countries where the mobility of population groups with secondary education is particularly affected by drought and aridity. This difference may be due to migration constraints among the lower-educated or reflect differential migration prospects for lower and higher-educated individuals (Levy & Wadycki, 1974; UNESCO, 2019). For more developed countries, while overall migration responses are more uniform across education groups, out-migration rates appear to be higher among groups with a primary level of education, although the very low number of individuals in this group results in large error bars.

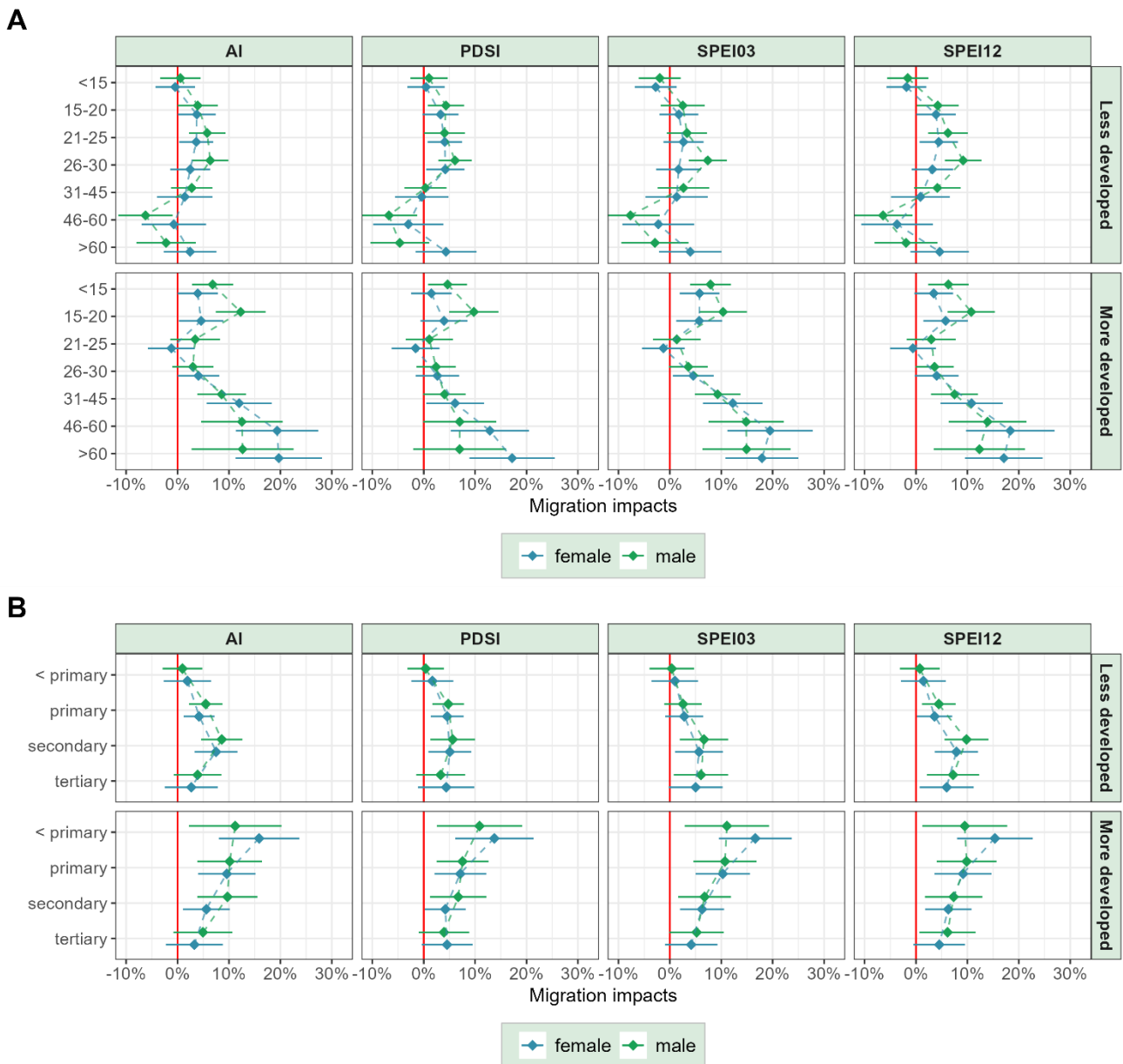


Figure 7. Migration impacts by different population subgroups in more and less developed countries.

Panel A shows estimated differences in migration responses for men (green dots and whiskers) and women (blue dots and whiskers) in different age groups (y-axis) for populations in more and less developed countries. Panel B shows differences in migration responses for men and women by ISCED education levels in more and less developed countries. The x-axis shows the marginal effects of a one standard deviation increase in drought and aridity measured with the four climate indicators. The classification into more and less developed countries is based on data from the UN World Population Prospects (UN, 2022).

Discussion and conclusion

Analyzing census-based migration data, our study shows significant and sizeable impacts of drought and aridity on internal migration worldwide. The effects are particularly pronounced in agriculturally dependent, rural regions, especially in drylands in Southern Europe, the Middle East and North Africa, Southern Asia, and North America. Economic prosperity and development also influence the relationships. Mobility tends to be higher in relatively poorer regions (compared to the country average) that are still wealthy enough to finance migration. Also, individual characteristics are found to play an important role in shaping migration responses. While mobility is higher among the better-educated working-age population in developing countries, we observe stronger impacts on the mobility for the older age groups across all education strata in wealthier countries. These findings highlight the importance of differing mobility patterns among distinct population groups in diverse contexts.

Our study adds to the growing body of literature emphasizing the important role of environmental factors in shaping (im)mobility outcomes (Beine & Jeusette, 2019; Cattaneo et al., 2019; Hoffmann et al., 2020; Hunter et al., 2015; Šedová et al., 2021). The relationships are not simple but are characterized by non-linearities (McLeman, 2018; Nawrotzki et al., 2017; Pasini & Amendola, 2019) and a high context dependency (Hoffmann, 2022; McLeman & Hunter, 2010; Upadhyay et al., 2015). Socio-economic conditions, political and cultural influences, and population characteristics can shape mobility responses to increased environmental stress (Black et al., 2011b, 2011a). These factors can lead to differences in migration patterns between, but also within countries, highlighting the need for a sub-national perspective to understand climate mobility and the role of local conditions (Muttarak, 2021).

Aside from spatial heterogeneity, our results reveal large differences in migration responses for different subgroups of the population. Both demographic and socio-economic characteristics can influence a person's ability and willingness to migrate, as well as the exposure and vulnerability to hazards (de Haas, 2021; de Sherbinin et al., 2022). Vulnerable communities, particularly those with limited resources and adaptive capacities, are likely to be disproportionately affected by environmental stress but may lack resources or information to engage in inter-regional migration (Cundill et al., 2021; Nawrotzki & DeWaard, 2018; Zickgraf & Perrin, 2016). Taking a holistic perspective that accounts for both spatial and social differences is key to comprehensively understanding the multifaceted links between the environment and human (im)mobility.

Advancements in data availability and modeling techniques have improved migration assessment and estimation. Despite these improvements, the limited availability and comparability of internal migration data pose considerable challenges to reflect mobility within countries accurately (Hoffmann et al., 2021; Vinke & Hoffmann, 2020). Inconsistent collection and reporting of data across regions and countries, gaps in the systematic collection of migration data, and a lack of standardized classifications and categories for internal migration make it challenging to establish consistent analytical frameworks and hinder efforts to compare migration patterns and trends across regions and countries over time. Consequently, it has been challenging to present consistent evidence to what extent and how climatic factors influence internal migration.

To that end, the longitudinal migration dataset extracted from the IPUMS census microdata can address some of these issues (Minnesota Population Center, 2020). Through extensive data harmonization and cleaning efforts, this dataset offers comparable information on migration across 72 countries, facilitating a systematic examination of geographic disparities in internal migration patterns. In addition to modeling climatic influences

on human mobility, the data can be utilized in various other relevant applications. While the data provide a comprehensive picture of global bilateral internal migration, they have limitations. In particular, certain forms of climate-related mobility, including short-distance and temporal migration, may be omitted from the analysis.

Our work contributes to the assessment of the impact of drought and aridity, which can have severe consequences for agricultural production, water security, and livelihoods, on internal migration patterns (Straffelini & Tarolli, 2023). As climate change continues to unfold, projections suggest an increase in the frequency and severity of arid conditions in various regions across the globe (Huang et al., 2016; Wang et al., 2021). Populations living in areas experiencing chronic water scarcity and agricultural challenges will likely face heightened pressures to seek alternative livelihoods and better living conditions elsewhere (Rigaud et al., 2018).

The findings that drier conditions lead to higher internal migration among subgroups of populations based on socio-economic characteristics present an empirical ground for targeted policies. Under elevated environmental stress, those who need to migrate but do not have the resources to do so would need support to facilitate migration and better means to protect themselves and their communities. Likewise, given the vital role of the rural-to-urban migration corridor, the challenge is to ensure adequate facilities, infrastructure, and social and health services in destination regions for a growing urban population (Hoffmann & Muttarak, 2021).

Proactive policy measures are needed to address challenges related to climate change and human mobility and to reduce vulnerabilities of communities affected by environmental stress (Blake et al., 2021; Thalheimer et al., 2022). Enhancing water management strategies, promoting resilient agricultural practices, and implementing climate adaptation measures can help mitigate the adverse effects of drought and aridity. Furthermore, policies that support livelihood diversification and social safety nets can assist in reducing forced migration and displacement, promote resilience in vulnerable communities, and support mobile populations.

References

- Abel, G. J., & Cohen, J. E. (2022). Bilateral international migration flow estimates updated and refined by sex. *Scientific Data* 2022 9:1, 9(1), 1–11. <https://doi.org/10.1038/s41597-022-01271-z>
- Abel, G. J., Muttarak, R., & Stephany, F. (2022). *Climatic Shocks and Internal Migration: Evidence from 442 Million Personal Records in 64 Countries* (168232; 1W-Water, Migration, And Development -- P173491). World Bank.
- Abel, G. J., & Sander, N. (2014). Quantifying global international migration flows. *Science*, 343(6178), 1520–1522. <https://doi.org/10.1126/science.1248676>
- Beguiría, S., Vicente-Serrano, S. M., & Angulo-Martínez, M. (2010). A Multiscalar Global Drought Dataset: The SPEIbase: A New Gridded Product for the Analysis of Drought Variability and Impacts. *Bulletin of the American Meteorological Society*, 91(10), 1351–1356. <https://doi.org/10.1175/2010BAMS2988.1>
- Beine, M., Bertoli, S., & Fernández-Huertas Moraga, J. (2016). A Practitioners' Guide to Gravity Models of International Migration. *World Economy*, 39(4), 496–512. <https://doi.org/10.1111/twec.12265>
- Beine, M., & Jeusette, L. (2019). A meta-analysis of the literature on Climate Change and Migration. *IZA Discussion Papers 12639 2018/05*, Art. 12639 2018/05.
- Beine, M., & Parsons, C. (2015). Climatic factors as determinants of international migration. *Scandinavian Journal of Economics*, 117(2), 723–767. <https://doi.org/10.1111/sjoe.12098>
- Bell, M., Charles-Edwards, E., Ueffing, P., Stillwell, J., Kupiszewski, M., & Kupiszewska, D. (2015). Internal Migration and Development: Comparing Migration Intensities Around the World. *Population and Development Review*, 41(1), 33–58. <https://doi.org/10.1111/J.1728-4457.2015.00025.X>
- Benveniste, H., Oppenheimer, M., & Fleurbaey, M. (2022). Climate change increases resource-constrained international immobility. *Nature Climate Change*, 12(7), 634–641. <https://doi.org/10.1038/s41558-022-01401-w>
- Bergé, L. R. (2018). Efficient estimation of maximum likelihood models with multiple fixed-effects: the R package FENmlm. *CREA Discussion Papers*, 13.
- Black, R., Adger, N., Arnell, N., Dercon, S., Geddes, A., & Thomas, D. (2011a). *Foresight: Migration and global environmental change. Future challenges and opportunities* [Final Project Report]. The Government Office for Science.
- Black, R., Adger, W. N., Arnell, N. W., Dercon, S., Geddes, A., & Thomas, D. (2011b). The effect of environmental change on human migration. *Global Environmental Change*, 21(SUPPL. 1), 3–11. <https://doi.org/10.1016/j.gloenvcha.2011.10.001>
- Blake, J. S., Clark-Ginsberg, A., & Balagna, J. (2021). *Addressing Climate Migration: A Review of National Policy Approaches*. RAND International. <https://www.rand.org/pubs/perspectives/PEA1085-1.html>
- Bohra-Mishra, P., Oppenheimer, M., Cai, R., Feng, S., & Licker, R. (2017). Climate variability and migration in the Philippines. *Population and Environment*, 38(3), 286–308. <https://doi.org/10.1007/s11111-016-0263-x>

- Borderon, M., Sakdapolrak, P., Muttarak, R., Kebede, E., Pagogna, R., & Sporer, E. (2019). Migration influenced by environmental change in Africa: A systematic review of empirical evidence. *Demographic Research*, *41*, 491–544. <https://doi.org/10.4054/DemRes.2019.41.18>
- Burrell, A. L., Evans, J. P., & de Kauwe, M. G. (2020). Anthropogenic climate change has driven over 5 million km² of drylands towards desertification. *Nature Communications*, *11*(1), 3853. <https://doi.org/10.1038/s41467-020-17710-7>
- Cattaneo, C., Beine, M., Fröhlich, C. J., Kniveton, D., Martinez-Zarzoso, I., Mastroiello, M., Millock, K., Piguet, E., & Schraven, B. (2019). Human Migration in the Era of Climate Change. *Review of Environmental Economics and Policy*, *rez008*, 1–19.
- Cirillo, M., Cattaneo, A., Miller, M., & Sadiddin, A. (2022). Establishing the link between internal and international migration: Evidence from Sub-Saharan Africa. *World Development*, *157*, 105943. <https://doi.org/10.1016/J.WORLDDEV.2022.105943>
- Clement, V., Rigaud, K. K., de Sherbinin, A., Jones, B., Adamo, S., Schewe, J., Sadiq, N., & Shabahat, E. (2021). *Groundswell Part 2: Acting on Internal Climate Migration*. World Bank.
- Cundill, G., Singh, C., Adger, W. N., Safra de Campos, R., Vincent, K., Tebboth, M., & Maharjan, A. (2021). Toward a climate mobilities research agenda: Intersectionality, immobility, and policy responses. *Global Environmental Change*, *69*, 102315. <https://doi.org/10.1016/j.gloenvcha.2021.102315>
- de Haas, H. (2021). A theory of migration: the aspirations-capabilities framework. *Comparative Migration Studies*, *9*(1). <https://doi.org/10.1186/s40878-020-00210-4>
- de Sherbinin, A., Grace, K., McDermid, S., van der Geest, K., Puma, M. J., & Bell, A. (2022). Migration Theory in Climate Mobility Research. *Frontiers in Climate*, *4*, 78. <https://doi.org/10.3389/fclim.2022.882343>
- Dell, M., Jones, B. F., & Olken, B. A. (2014). What do we learn from the weather? The new climate-economy literature. *Journal of Economic Literature*, *52*(3), 740–798. <https://doi.org/10.1257/jel.52.3.740>
- Dow, K., Berkhout, F., & Preston, B. L. (2013). Limits to adaptation to climate change: A risk approach. In *Current Opinion in Environmental Sustainability* (Vol. 5, Issues 3–4, pp. 384–391). Elsevier. <https://doi.org/10.1016/j.cosust.2013.07.005>
- European Commission/Joint Research Centre. (2018). *World atlas of desertification – Rethinking land degradation and sustainable land management* (J. Hill, G. Von Maltitz, S. Sommer, J. Reynolds, C. Hutchinson, & M. Cherlet, Eds.). European Commission Publications Office.
- FAO. (2019). Trees, forests and land use in drylands: the first global assessment. In *Food and Agriculture Organization of the United Nations. Forestry Paper No. 184*. <http://www.fao.org/documents/card/en/c/ca7148en/>
- Farbotko, C., Dun, O., Thornton, F., McNamara, K. E., & McMichael, C. (2020). Relocation planning must address voluntary immobility. *Nature Climate Change*, *10*(8), 702–704. <https://doi.org/10.1038/s41558-020-0829-6>
- Garcia, A. J., Pindolia, D. K., Lopiano, K. K., & Tatem, A. J. (2015). Modeling internal migration flows in sub-Saharan Africa using census microdata. *Migration Studies*, *3*(1), 89–110. <https://doi.org/10.1093/migration/mnu036>

- Gray, C., & Mueller, V. (2012). Drought and Population Mobility in Rural Ethiopia. *World Development*, 40(1), 134–145. <https://doi.org/10.1016/j.worlddev.2011.05.023>
- Harris, I., Osborn, T. J., Jones, P., & Lister, D. (2020). Version 4 of the CRU TS monthly high-resolution gridded multivariate climate dataset. *Scientific Data*, 7(1), 1–18. <https://doi.org/10.1038/s41597-020-0453-3>
- Henderson, J. V., Storeygard, A., & Deichmann, U. (2017). Has climate change driven urbanization in Africa? *Journal of Development Economics*, 124, 60–82. <https://doi.org/10.1016/j.jdevco.2016.09.001>
- Hoffmann, R. (2022). Contextualizing Climate Change Impacts on Human Mobility in African Drylands. *Earth's Future*, 10(6), e2021EF002591. <https://doi.org/10.1029/2021EF002591>
- Hoffmann, R., Dimitrova, A., Muttarak, R., Crespo Cuaresma, J., & Peisker, J. (2020). A Meta-Analysis of Country Level Studies on Environmental Change and Migration. *Nature Climate Change*, 10, 904–912. <https://doi.org/https://doi.org/10.1038/s41558-020-0898-6>
- Hoffmann, R., & Muttarak, R. (2021). *Environment, migration and urbanisation: challenges and solutions for low- and middle-income countries*. https://www.g20-insights.org/policy_area/youth-aging-population-migration/
- Hoffmann, R., Šedová, B., & Vinke, K. (2021). Improving the Evidence Base on Climate Migration: Methodological Insights from Two Meta-Analyses. *Global Environmental Change*, 71, 102367.
- Hoffmann, R., Wiederkehr, C., Dimitrova, A., & Hermans, K. (2022). Agricultural livelihoods, adaptation, and environmental migration in sub-Saharan drylands: A meta-analytical review. *Environmental Research Letters*, 17(8). <https://doi.org/10.1088/1748-9326/ac7d65>
- Hsiang, S. (2016). Climate Econometrics. *Annual Review of Resource Economics*, 8(1), 43–75. <https://doi.org/10.1146/annurev-resource-100815-095343>
- Huang, J., Yu, H., Guan, X., Wang, G., & Guo, R. (2016). Accelerated dryland expansion under climate change. *Nature Climate Change*, 6(2), 166–171. <https://doi.org/10.1038/nclimate2837>
- Hunter, L. M., Luna, J. K., & Norton, R. M. (2015). Environmental Dimensions of Migration. *Annual Review of Sociology*, 41, 377–397. <https://doi.org/10.1146/annurev-soc-073014-112223>
- Kummu, M., Taka, M., & Guillaume, J. H. A. (2018). Gridded global datasets for Gross Domestic Product and Human Development Index over 1990–2015. *Scientific Data* 2018 5:1, 5(1), 1–15. <https://doi.org/10.1038/sdata.2018.4>
- Lerch, M. (2020). International Migration and City Growth in the Global South: An Analysis of IPUMS Data for Seven Countries, 1992–2013. *Population and Development Review*, 46(3), 557–582. <https://doi.org/10.1111/PADR.12344>
- Levy, M. B., & Wadycski, W. J. (1974). Education and the Decision to Migrate: An Econometric Analysis of Migration in Venezuela. *Econometrica*, 42(2), 377. <https://doi.org/10.2307/1911985>
- Mallick, B., & Schanze, J. (2020). Trapped or Voluntary? Non-Migration Despite Climate Risks. *Sustainability*, 12(11), 4718. <https://doi.org/10.3390/su12114718>
- Manning, P., & Trimmer, T. (2020). *Migration in world history*. Routledge.
- Marchiori, L., Maystadt, J. F., & Schumacher, I. (2017). Is environmentally-induced income variability a driver of migration? *Migration and Development*, 6(1), 33–59. <https://doi.org/10.1080/21632324.2015.1020106>

- McLeman, R. (2018). Thresholds in climate migration. *Population and Environment*, 39(4), 319–338. <https://doi.org/10.1007/s11111-017-0290-2>
- McLeman, R. A., & Hunter, L. M. (2010). Migration in the context of vulnerability and adaptation to climate change: Insights from analogues. *Wiley Interdisciplinary Reviews: Climate Change*, 1(3), 450–461. <https://doi.org/10.1002/wcc.51>
- McLeman, R., & Smit, B. (2006). Migration as an adaptation to climate change. *Climatic Change*, 76(1–2), 31–53. <https://doi.org/10.1007/s10584-005-9000-7>
- Mendelsohn, R. (2008). The Impact of Climate Change on Agriculture in Developing Countries. *Journal of Natural Resources Policy Research*, 1(1), 5–19. <https://doi.org/10.1080/19390450802495882>
- Meze-Hausken, E. (2008). On the (im-)possibilities of defining human climate thresholds. *Climatic Change*, 89(3–4), 299–324.
- Minnesota Population Center. (2020). *Integrated Public Use Microdata Series, International: Version 7.2 [dataset]*. University of Minnesota. Minneapolis, MN. <https://international.ipums.org/international/>
- Mueller, V., Gray, C., & Kosec, K. (2014). Heat stress increases long-term human migration in rural Pakistan. *Nature Climate Change* 2014 4:3, 4(3), 182–185. <https://doi.org/10.1038/nclimate2103>
- Muttarak, R. (2021). Demographic perspectives in research on global environmental change. *Population Studies*, 75(S1), 77–104. <https://doi.org/10.1080/00324728.2021.1988684>
- Nawrotzki, R. J., & DeWaard, J. (2018). Putting trapped populations into place: climate change and inter-district migration flows in Zambia. *Regional Environmental Change*, 18(2), 533–546. <https://doi.org/10.1007/s10113-017-1224-3>
- Nawrotzki, R. J., DeWaard, J., Bakhtsiyarava, M., & Ha, J. T. (2017). Climate shocks and rural-urban migration in Mexico: exploring nonlinearities and thresholds. *Climatic Change*, 140(2), 243–258. <https://doi.org/10.1007/s10584-016-1849-0>
- Niva, V., Kallio, M., Muttarak, R., Taka, M., Varis, O., & Kummu, M. (2021). Global migration is driven by the complex interplay between environmental and social factors. *Environmental Research Letters*, 16(11), 114019. <https://doi.org/10.1088/1748-9326/ac2e86>
- Pasini, A., & Amendola, S. (2019). Linear and nonlinear influences of climatic changes on migration flows: A case study for the 'mediterranean bridge.' *Environmental Research Communications*, 1(1). <https://doi.org/10.1088/2515-7620/ab0464>
- Pörtner, H., Roberts, D., Tignor, M., Poloczanska, E., Mintenbeck, K., Alegría, A., Craig, M., Langsdorf, S., Löschke, S., Möller, V., Okem, A., Rama, B., Adams, H., Adelekan, I., Adler, C., Adrian, R., Aldunce, P., Ali, E., Ara Begum, R., ... Sukumar, R. (2022). *Climate Change 2022: Impacts, Adaptation and Vulnerability Working Group II Contribution to the Sixth Assessment Report of the Intergovernmental Panel on Climate Change*. <https://doi.org/10.1017/9781009325844.Front>
- Rigaud, K. K., Sherbinin, A. de, Jones, B., Bergmann, J., Clement, V., Ober, K., Schewe, J., Adamo, S., McCusker, B., Heuser, S., & Midgley, A. (2018). *Groundswell - Preparing for internal climate migration*. World Bank. <https://doi.org/doi.org/10.7916/D8Z33FNS>

- Santos Silva, J. M. C., & Tenreyro, S. (2006). The log of gravity. *Review of Economics and Statistics*, 88(4), 641–658. <https://doi.org/10.1162/rest.88.4.641>
- Savaş, E. B., Spaan, J., Henkens, K., Kalmijn, M., & Dalen, H. P. van. (2023). Migrating to a new country in late life: A review of the literature on international retirement migration. *Demographic Research*, 48, 233–270. <https://doi.org/10.4054/DEMRES.2023.48.9>
- Schlenker, W., & Lobell, D. B. (2010). Robust negative impacts of climate change on African agriculture. *Environmental Research Letters*, 5(1). <https://doi.org/10.1088/1748-9326/5/1/014010>
- Šedová, B., Čizmaziová, L., & Cook, A. (2021). A meta-analysis of climate migration literature. *CEPA Discussion Papers*, 29.
- Straffelini, E., & Tarolli, P. (2023). Climate change-induced aridity is affecting agriculture in Northeast Italy. *Agricultural Systems*, 208, 103647. <https://doi.org/10.1016/J.AGSY.2023.103647>
- Thalheimer, L., Simperingham, E., & Jjemba, E. W. (2022). The role of anticipatory humanitarian action to reduce disaster displacement. *Environmental Research Letters*, 17(1), 014043. <https://doi.org/10.1088/1748-9326/ac4292>
- Thiede, B. C., Robinson, A., & Gray, C. (2022). *Climatic Variability and Internal Migration in Asia: Evidence from Integrated Census and Survey Microdata*. file:///C:/Users/hoffmannr/Downloads/Thiede_Robinson_Gray_WP.pdf
- UN. (2022). *2022 Revision of World Population Prospects*. <https://population.un.org/wpp/>
- UNESCO. (2019). International Migration. In *Global Education Monitoring Report*. <https://gem-report-2019.unesco.org/chapter/introduction/international-migration/>
- Upadhyay, H., Kelman, I., Lingaraj, G. J., Mishra, A., Shreve, C., & Stojanov, R. (2015). Conceptualizing and contextualizing research and policy for links between climate change and migration. *International Journal of Climate Change Strategies and Management*, 7(3), 394–417. <https://doi.org/10.1108/IJCCSM-05-2014-0058>
- Vinke, K., & Hoffmann, R. (2020). Data for a difficult subject: Climate change and human migration. *Migration Policy Practice*, forthcoming.
- Wang, X., Jiang, D., & Lang, X. (2021). Future changes in Aridity Index at two and four degrees of global warming above preindustrial levels. *International Journal of Climatology*, 41(1), 278–294. <https://doi.org/10.1002/JOC.6620>
- Warner, K., Geest, K. Van Der, Kreft, S., Huq, S., Harmeling, S., Kusters, K., & Sherbinin, A. De. (2012). Evidence from the frontlines of climate change: Loss and damage to communities despite coping and adaptation. *Report*, 9(9), 1–86.
- Zickgraf, C., & Perrin, N. (2016). Immobile and trapped populations. In F. Gemenne, D. Ionesco, & D. Mokhnacheva (Eds.), *The Atlas of Environmental Migration*. Routledge.

Supplementary Materials

Extended descriptive statistics

Figures S1 to S4 show temporal trends in the drought and aridity indicators for the different world regions considered in our analysis. Table S1 provides summary statistics for the main population variables used in our analysis, including the different migration measures. Table S2 shows summary statistics for the drought and aridity indicators. Table S3 presents background statistics for the 72 countries included in the analysis.

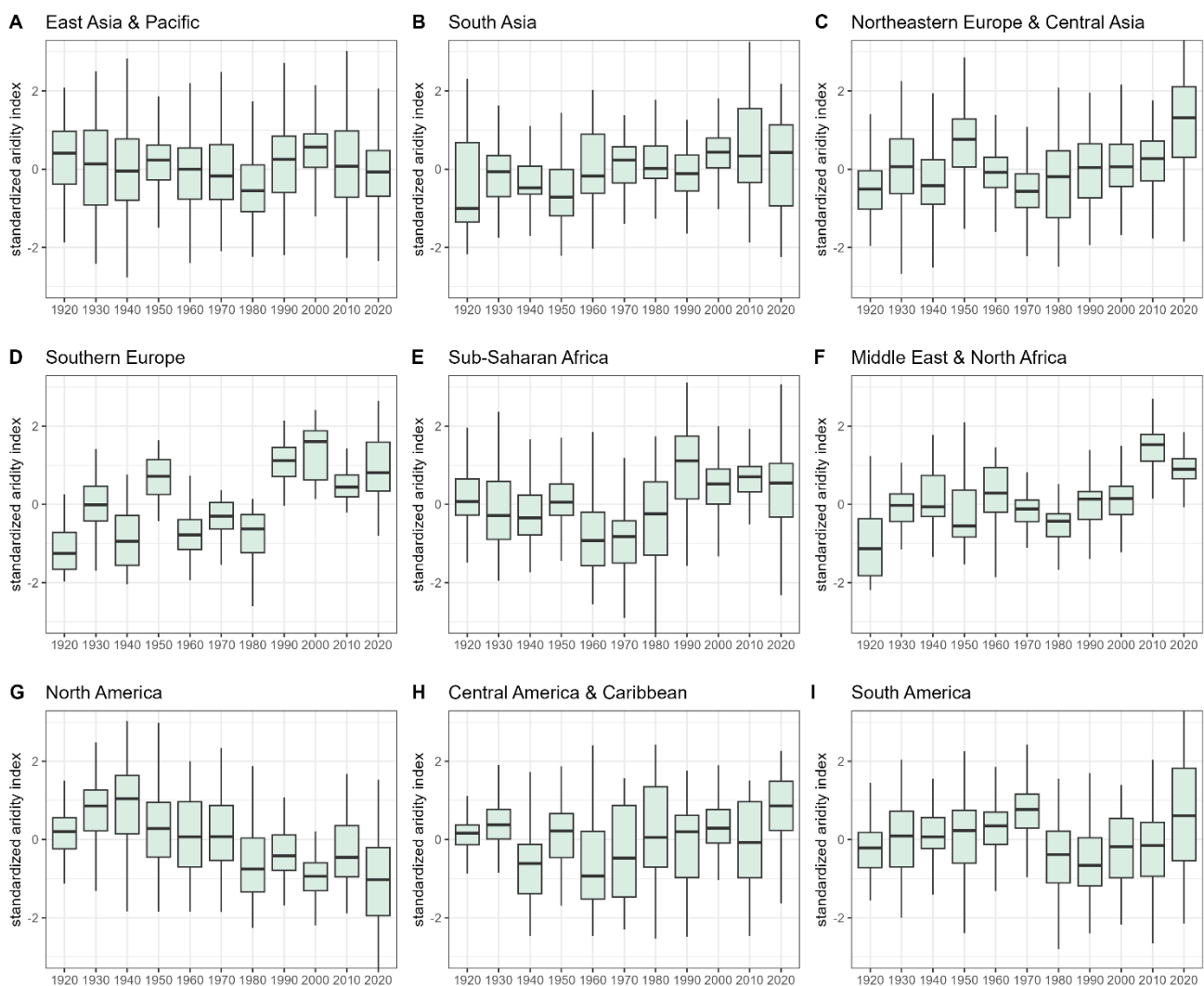


Figure S1. Temporal trends in the standardized aridity index (AI) 1920 – 2020 by world regions.

The boxplots show the median, interquartile ranges (IQR), and $1.5 \times \text{IQR}$ of the distribution across subnational regions. Only countries covered in the migration data are included in the calculation. The original AI was rescaled so that positive values indicate greater and negative values reduced dryness.

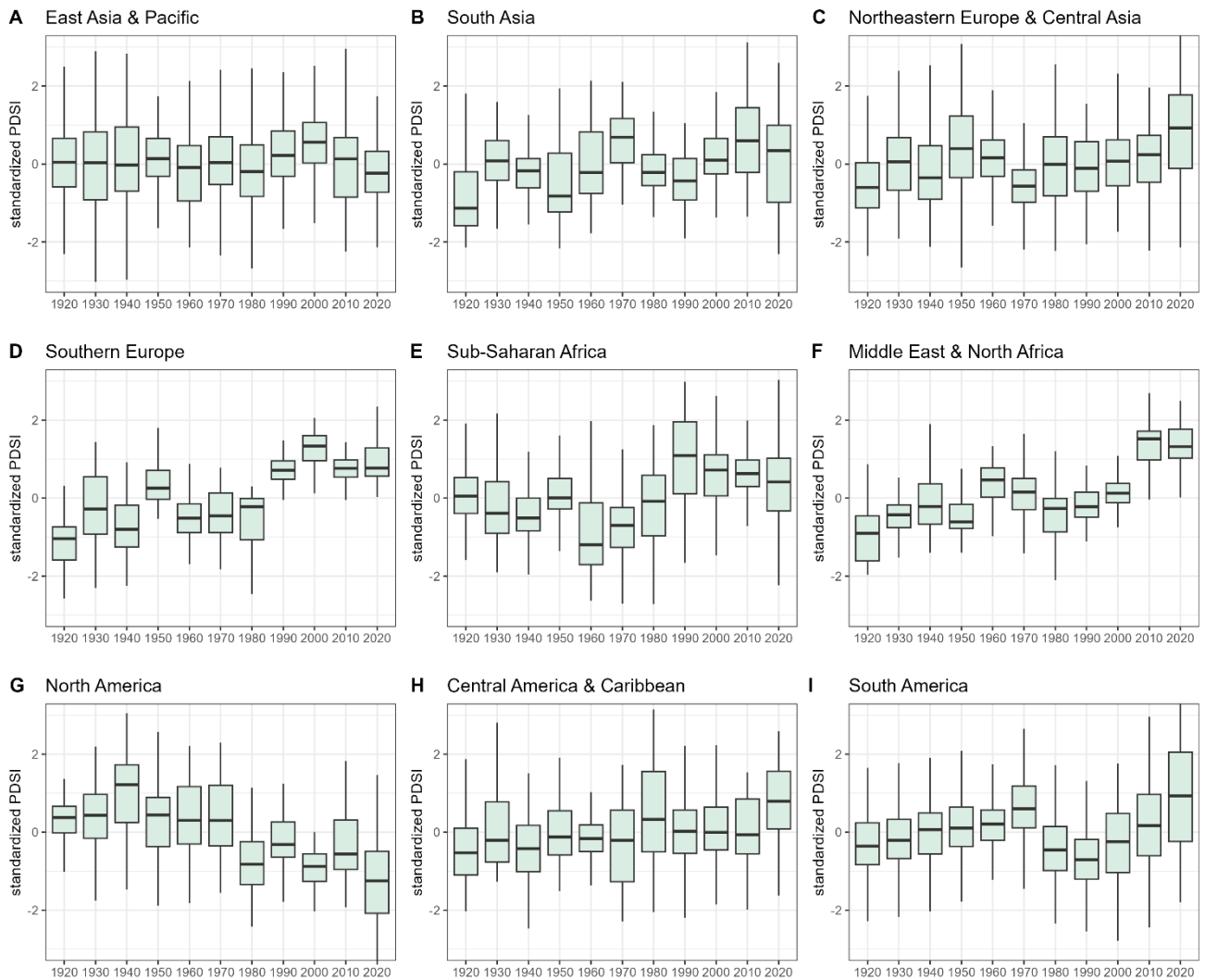


Figure S2. Temporal trends in the standardized Palmer Drought Severity Index (PDSI) 1920 – 2020 by world regions.

The boxplots show the median, interquartile ranges (IQR), and 1.5 x IQR of the distribution across subnational regions. Only countries covered in the migration data are included in the calculation. The original PDSI was rescaled so that positive values indicate greater and negative values reduced dryness.

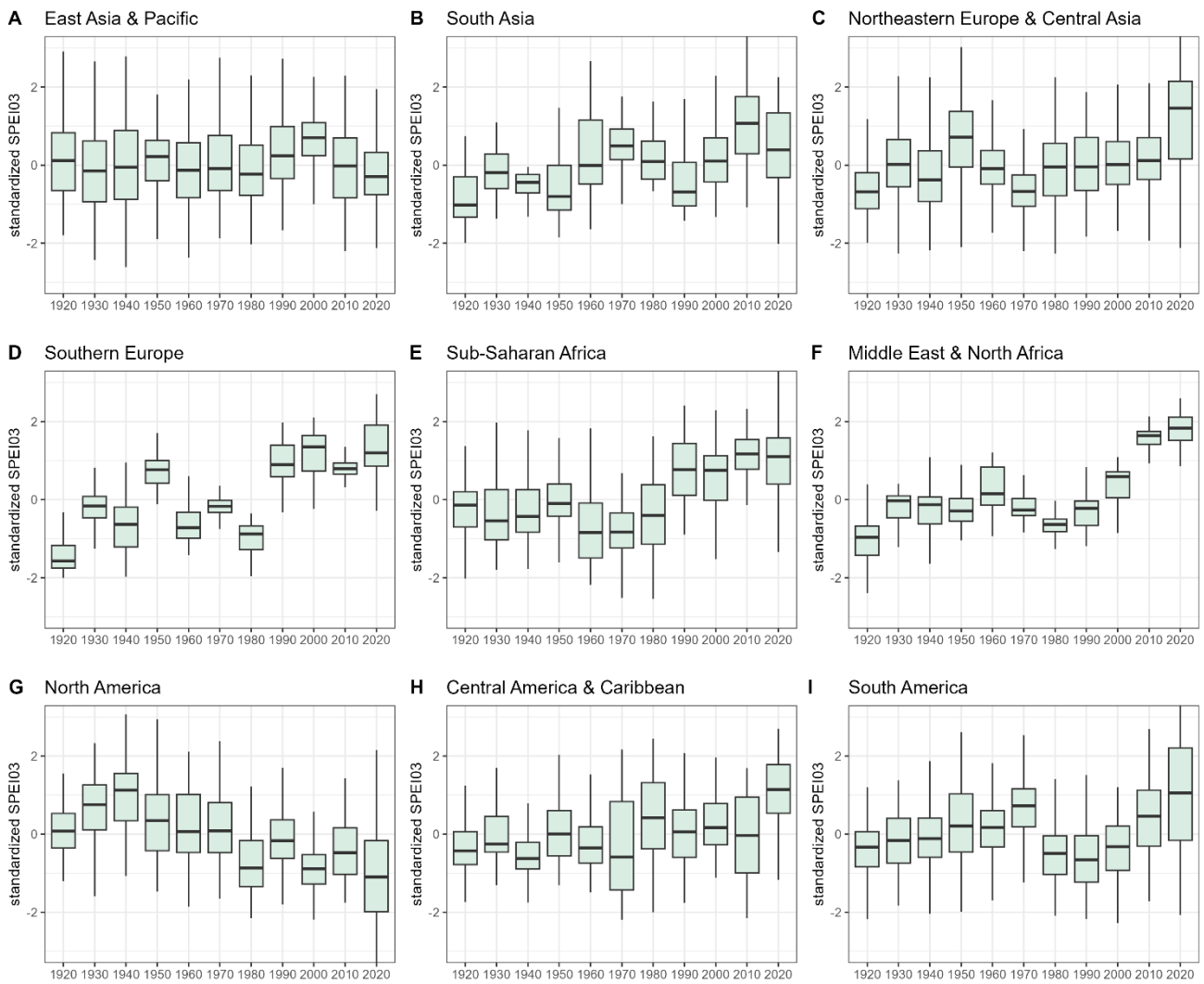


Figure S3. Temporal trends in the standardized Standardized Precipitation Evapotranspiration Index measured over a three months time window (SPEI03) 1920 – 2020 by world regions.

The boxplots show the median, interquartile ranges (IQR), and $1.5 \times \text{IQR}$ of the distribution across subnational regions. Only countries covered in the migration data are included in the calculation. The original SPEI03 was rescaled so that positive values indicate greater and negative values reduced dryness.

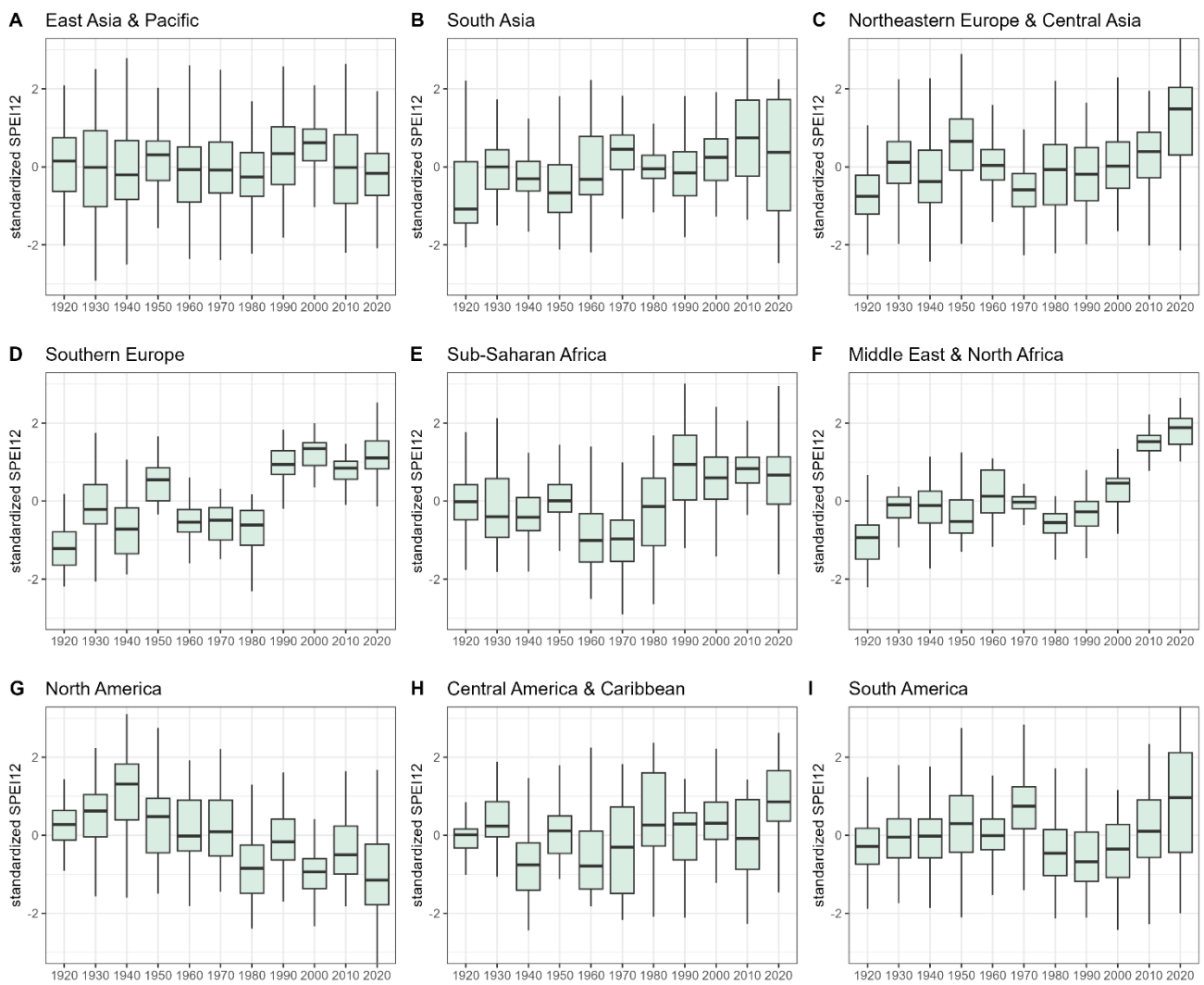


Figure S4. Temporal trends in the standardized Standardized Precipitation Evapotranspiration Index measured over a 12 months time window (SPEI12) 1920 – 2020 by world regions.

The boxplots show the median, interquartile ranges (IQR), and $1.5 \times \text{IQR}$ of the distribution across subnational regions. Only countries covered in the migration data are included in the calculation. The original SPEI12 was rescaled so that positive values indicate greater and negative values reduced dryness.

Table S2 – Summary of variables at the subnational regional level

	Less developed economies				
	N	Mean	SD	Min	Max
Migration					
Annual out-migration rate	3192	0.014	0.055	0	2.543
Annual out-migration flow	3192	15309	39613	3	103726
Migration interval 1 year	3192	0.084	0.277	0	1
Migration interval 5 years	3192	0.916	0.277	0	1
Population & geography					
Population in origin region	3192	3042513.37	9876053.81	9060	160415922
Area of origin region	2968	50445516	135917675	12437.96	1632612236
Origin region has coastal border	2968	0.489	0.5	0	1
Origin region has land border	2968	0.438	0.496	0	1
Origin region has no border	2968	0.228	0.42	0	1
Population density (per 1000km ²)	2968	0.362	1.954	0	44.003
Number of destination regions	3192	30.649	19.916	3	76
Distance origin to destination	3192	591225	474370	17521	2883161
Destination is adjacent	3192	0.212	0.16	0	1
Socioeconomic background					
Unemployment rate	2499	0.050	0.059	0.000	0.525
GDP per capita	2135	6592	6472	260	105303
HDI	2135	0.594	0.121	0.267	0.969
Share agricultural employment	2794	0.455	0.262	0.003	0.97
Share urban	2567	0.42	0.288	0	1
Country GINI coefficient	3115	0.422	0.06	0.297	0.63
Country % crop land	3182	0.392	0.168	0.005	0.873
Country GDP per capita	3185	2261	2890	76	15046
More developed economies					
	N	Mean	SD	Min	Max
Migration					
Annual out-migration rate	1075	0.025	0.077	0.001	1.504
Annual out-migration flow	1075	42577	81929	238	732686
Migration interval 1 year	1075	0.58	0.494	0	1
Migration interval 5 years	1075	0.42	0.494	0	1
Population & geography					
Population in origin region	1075	2371531.25	4276953.86	18830	39144818
Area of origin region	1075	107056980	305305205	13988.634	3944158051
Origin region has coastal border	1075	0.529	0.499	0	1
Origin region has land border	1075	0.302	0.459	0	1
Origin region has no border	1075	0.3	0.458	0	1
Population density (per 1000km ²)	1075	0.207	0.863	0	10.463
Number of destination regions	1075	44.171	19.051	4	82
Distance origin to destination	1075	1002283	998742	66086	6403459

Destination is adjacent	1075	0.149	0.146	0	1
Socioeconomic background					
Unemployment rate	1034	0.066	0.044	0.006	0.415
GDP per capita	787	29885	18008	2124	182907
HDI	787	0.815	0.077	0.452	0.955
Share agricultural employment	984	0.157	0.177	0	0.762
Share urban	409	0.56	0.207	0.025	1
Country GINI coefficient	1075	0.364	0.043	0.246	0.63
Country % crop land	1075	0.512	0.176	0.068	0.82
Country GDP per capita	1038	19250	16390	1102	56763

Table S3 - Summary of aridity and drought indicators

	N	Mean	SD	Min	Max
Subnational standardization					
AI averaged over 10 years	4267	0.019	1.042	-3.802	3.167
SPEI03 averaged over 10 years	4267	0.119	1.041	-3.824	2.832
SPEI12 averaged over 10 years	4267	0.085	1.039	-3.693	3.122
PDSI averaged over 10 years	4267	0.083	1.028	-3.673	2.71
Country-level standardization					
AI averaged over 10 years	4267	0.009	0.999	-4.057	2.785
SPEI03 averaged over 10 years	4267	0.121	1.053	-4.738	3.445
SPEI12 averaged over 10 years	4267	0.086	1.044	-4.44	3.591
PDSI averaged over 10 years	4267	0.076	0.984	-3.677	3.167
Global standardization					
AI averaged over 10 years	4267	0.049	0.951	-5.181	2.196
SPEI03 averaged over 10 years	4267	0.14	1.067	-3.664	4.709
SPEI12 averaged over 10 years	4267	0.096	1.044	-3.285	3.733
PDSI averaged over 10 years	4267	0.09	0.928	-2.801	3.016
No standardization					
AI averaged over 10 years	4267	1.172	0.672	0.009	4.691
SPEI03 averaged over 10 years	4267	-0.029	0.246	-1.142	0.842
SPEI12 averaged over 10 years	4267	-0.031	0.389	-1.386	1.137
PDSI averaged over 10 years	4267	-0.278	1.05	-3.557	2.61

Table S4 – Overview of countries included in the bilateral migration database

#	Country name	World region	Max year	Min year	Distinct censuses	Number regions	Average distance	Adjacent regions	Area size
1	Argentina	South America	2001	1970	3	24	1139441	0.16	115813204
2	Armenia	Northeastern Europe & Central Asia	2011	2001	2	11	100263.6	0.38	2593559
3	Belarus	Northeastern Europe & Central Asia	1999	1999	1	6	253817.8	0.67	34600157
4	Benin	Sub-Saharan Africa	2013	1979	4	12	235205	0.30	9607942
5	Bolivia	South America	2012	1976	4	9	570850.6	0.44	120066351
6	Botswana	Sub-Saharan Africa	2011	1981	4	21	387926.1	0.20	27531437
7	Brazil	South America	2010	1970	5	25	1771232	0.15	339183618
8	Cambodia	East Asia & Pacific	2013	2004	3	21	203337.7	0.28	8525248
9	Cameroon	Sub-Saharan Africa	2005	1976	3	7	352001.4	0.57	66449854
10	Canada	North America	2001	1981	3	10	2090917	0.31	989833410
11	Chile	South America	2017	1982	4	42	859555.4	0.08	17066290
12	China	East Asia & Pacific	2000	1990	2	29	1457587	0.16	323533448
13	Colombia	South America	1973	1964	2	21	535011.2	0.22	54122108
14	Costa Rica	Central America	2011	1963	5	7	120637.7	0.57	7336134
15	Cuba	Caribbean	2012	2012	1	14	365978.9	0.19	110860
16	Dominican Republic	Caribbean	2010	1981	2	23	125432.7	0.22	2090818
17	Ecuador	South America	2010	1962	5	14	263956.6	0.34	18289510
18	Egypt, Arab Rep.	Middle East & North Africa	2006	1996	2	12	308028.9	0.19	20994608
19	El Salvador	Central America	2007	1992	2	14	85547.93	0.30	1482132
20	Fiji	East Asia & Pacific	2007	1976	4	4	368433.8	0.17	4762085
21	Ghana	Sub-Saharan Africa	2000	2000	1	10	301479.2	0.40	23909277
22	Greece	Southern Europe	2011	1971	5	54	283686	0.09	2462101
23	Guatemala	Central America	2002	1964	5	22	140494.5	0.23	4915813
24	Guinea	Sub-Saharan Africa	2014	1996	2	33	296337.7	0.16	7815534
25	Haiti	Caribbean	2003	1971	3	4	143785.8	0.67	6785627
26	Honduras	Central America	2001	1974	3	18	184386.3	0.25	6233781
27	India	South Asia	1999	1983	3	30	1031018	0.28	32870000
28	Indonesia	East Asia & Pacific	2010	1971	9	26	1414599	0.08	72819849
29	Ireland	Northeastern Europe & Central Asia	2011	1981	7	6	146255.7	0.53	8315782
30	Israel	Middle East & North Africa	1983	1983	1	7	88972.81	0.52	3847195
31	Jamaica	Caribbean	2001	1982	3	14	75782.78	0.28	785653
32	Kenya	Sub-Saharan Africa	2009	1979	4	8	354155.8	0.46	71834085
33	Kyrgyz Republic	Northeastern Europe & Central Asia	1999	1999	1	8	287683.5	0.40	24789651
34	Malawi	Sub-Saharan Africa	2008	2008	1	26	262594.4	0.16	3700823
35	Malaysia	East Asia & Pacific	2000	1991	2	13	612142.9	0.23	25372327
36	Mali	Sub-Saharan Africa	2009	1998	2	8	612685.4	0.32	156549298
37	Mauritius	Sub-Saharan Africa	2011	1990	3	10	125886.9	0.38	2040000

38	Mexico	Central America	2015	1960	8	32	902341.2	0.14	61158624
39	Mongolia	East Asia & Pacific	2000	2000	1	21	614336.6	0.27	74519559
40	Morocco	Middle East & North Africa	2004	2004	1	11	579566.8	0.19	28578884
41	Mozambique	Sub-Saharan Africa	2007	1997	2	11	751620.1	0.29	70889809
42	Myanmar	East Asia & Pacific	2014	2014	1	15	501112.2	0.28	676.578
43	Nepal	South Asia	2011	2001	2	14	300159	0.23	10570495
44	Nicaragua	Central America	2005	1971	3	12	160855.5	0.35	9982357
45	Panama	Central America	1980	1960	2	7	195184.5	0.55	10685146
46	Papua New Guinea	East Asia & Pacific	1990	1980	2	19	502504.1	0.21	23899152
47	Paraguay	South America	2002	1972	4	13	252762.4	0.36	30737910
48	Peru	South America	2007	2007	1	24	699348.1	0.18	53632401
49	Philippines	East Asia & Pacific	2010	1990	3	76	461807.3	0.06	3882933
50	Poland	Northeastern Europe & Central Asia	2002	2002	1	16	299225.2	0.29	19499181
51	Portugal	Southern Europe	2011	1981	4	22	394716.7	0.17	4186613
52	Romania	Northeastern Europe & Central Asia	2002	1977	3	39	247513.4	0.13	6096120
53	Russian Federation	Northeastern Europe & Central Asia	2010	2010	1	81	2021745	0.09	198113150
54	Senegal	Sub-Saharan Africa	2013	1988	3	8	239284.8	0.39	9386346
55	Sierra Leone	Sub-Saharan Africa	2015	2015	1	14	148234.5	0.29	5177310
56	Slovenia	Northeastern Europe & Central Asia	2002	2002	1	12	87010.38	0.33	1689843
57	South Africa	Sub-Saharan Africa	2016	2001	4	4	543652.4	0.83	304837868
58	South Sudan	Sub-Saharan Africa	2008	2008	1	10	443712.2	0.43	65288821
59	Spain	Southern Europe	2011	1991	2	19	590888.8	0.18	26646977
60	Sudan	Sub-Saharan Africa	2008	2008	1	15	684003	0.28	124020614
61	Suriname	South America	2012	2012	1	7	151449.2	0.51	16381900
62	Tanzania	Sub-Saharan Africa	2012	2002	2	23	511176.4	0.16	39163522
63	Thailand	East Asia & Pacific	2000	1970	4	68	386388.2	0.14	7560669
64	Togo	Sub-Saharan Africa	2010	2010	1	3	308371.8	0.67	18947004
65	Trinidad and Tobago	Caribbean	2000	1990	2	4	75922.74	0.33	1295045
66	Uganda	Sub-Saharan Africa	2014	2014	1	35	291360.2	0.05	5412941
67	United Kingdom	Northeastern Europe & Central Asia	2001	1991	2	12	302832.4	0.30	20479131
68	United States	North America	2015	1970	7	51	1871185	0.10	182849519
69	Uruguay	South America	2011	1975	5	19	221609.7	0.25	9354044
70	Venezuela, RB.	South America	2001	1981	2	22	470483.3	0.20	41459567
71	Vietnam	East Asia & Pacific	2009	1989	3	38	619237.4	0.10	8634385
72	Zambia	Sub-Saharan Africa	2010	1990	3	8	463674	0.43	93886583

Further results and extended analyses

This section presents additional results and extended analyses, which add further insights to the baseline models on the migration impacts of increased drought and aridity. The extended models also explore heterogeneities in the effects across different regions and by regional background characteristics.

Table S4 provides a cross-sectional perspective on the correlates of high out-migration rates at the regional level. Table S5 provides estimates of changes in migration flows over the past decades, which serve as a basis for Figure 4B in the main text. Table S6 explores non-linear patterns in drought and aridity impacts on migration by including quadratic terms of the climatic indicators in the estimation. The results reveal growing marginal effects suggesting rising migration pressures with increasing drought and aridity.

Table S7 shows heterogeneity in the migration impacts of drought and aridity for different world regions. The estimated coefficients and confidence intervals are displayed in Figure 5A in the main text. Table S8 further extends the model by controlling for different ecological zones, distinguishing hyper-arid/arid, semi-arid/sub-humid, and humid areas. The estimates from this model are used in combination with the information on projected changes in aridity to derive the explorative prediction of drought and aridity impacts on migration globally. Figure S5 shows projected changes in the aridity index using data from (Wang et al., 2021). The projected changes are used in combination with the results depicted in Table S8 to provide an explorative prediction of potential migration responses to increased drought and aridity in different parts of the world. The results of this prediction exercise are displayed in Figure 5B.

Figure S6 illustrates the role of country background characteristics in shaping migration responses to drought and aridity. It corresponds to Figure 6A in the main text, which shows the heterogeneity in marginal effects on migration by region characteristics. The country-level heterogeneity shown here confirms the findings on the regional differences and adds further insights, e.g., regarding the role of inequality. Here, we find weaker migration responses to drought and aridity in regions with an overall higher inequality as measured with the Gini coefficient under control for the GDP per capita in the country.

Tables S9 to S14 show interaction models exploring the role of regional characteristics in influencing migration responses to drought and aridity. The models consider interactions between the climate indicators and the GDP per capita, the agricultural employment share, and the urban population share in the regions of origin (Tables S9-S11) as well as with regional deviations in GDP per capita, agricultural employment, and urban population share from the country-specific mean (Tables S12-S14). The regional deviations were standardized to allow for comparisons across countries. Considering standardized deviations as opposed to the overall level values of the variables allows testing for differences in migration responses by within-country differences in wealth, agricultural dependency, and urban population. The tables are the basis of Figure 6 in the main text.

Tables S15 and S16 show further falsification tests and sensitivity analyses. In addition to the historic climate variables, the models displayed in Table S15 control for the lead values of the climate indicators in the period ten years after the census. None of these are found to significantly influence migration patterns. At the same time, the results for the historic impacts remain robust, suggesting that past experiences of environmental changes and stress lead to greater out-migration from affected regions. In addition to analyzing changes in

climatic conditions in origin regions, models in Table S16 show the impact of climatic conditions in destination regions on migration flows between origin and destination region pairs.

Table S5 – Extended models: Migration drivers in a cross-sectional comparison

	Outcome variable: Annual bilateral out-migration rate					
	(1)	(2)	(3)	(4)	(5)	(6)
Constant	0.0003 (0.0004)	0.0042*** (0.0006)	0.0045*** (0.0006)	0.0053*** (0.0014)	0.0042*** (0.0011)	0.0021*** (0.0004)
Migration interval 5 years	-0.0003*** (0.0001)	-0.0002*** (0.0001)	-0.0002*** (0.0001)	-0.0002*** (0.0001)	-0.0017*** (0.0002)	-0.0002*** (0.0001)
Number of destination regions	0.0001* (0.0001)	0.0001 (0.0001)	0.0001 (0.0001)	0.0001 (0.0001)	0.0001 (0.0001)	0.0001 (0.0001)
Log(distance)		-0.0003*** (0.0001)	-0.0003*** (0.0001)	-0.0003*** (0.0001)	-0.0003*** (0.0001)	-0.0003*** (0.0001)
Neighboring origin and destination		0.0009*** (0.0001)	0.0009*** (0.0001)	0.0010*** (0.0001)	0.0009*** (0.0001)	0.0009*** (0.0001)
Origin has land border			0.0003*** (0.0001)	0.0003*** (0.0001)	0.0004*** (0.0001)	0.0003*** (0.0001)
Destination has land border			-0.0001*** (0.0001)	0.0001 (0.0001)	0.0001 (0.0001)	-0.0001*** (0.0001)
Origin GDP per capita				0.0001 (0.0001)		
Origin agricultural employment				-0.0003*** (0.0001)		
Destination GDP per capita				0.0001*** (0.0001)		
Destination agricultural employment				-0.0016*** (0.0001)		
Origin urban population share					-0.0004 (0.0003)	
Destination urban population share					0.0024*** (0.0002)	
Gini coefficient (country-level)						0.0056*** (0.0019)
Observations	107,916	107,916	102,880	65,711	66,099	101,998
R2	0.06447	0.06946	0.06985	0.05515	0.06636	0.06986
Adj. R2	0.0638	0.06877	0.06915	0.05416	0.06534	0.06915

Note: Linear Ordinary Least Squares (OLS) models. Regression coefficients with heterogeneity robust standard errors in parentheses. The sample size of the models varies due to changes in the availability of variables in the IPUMS census data. The outcome variable is the annual out-migration rate. P-values: * 0.1 ** 0.05 *** 0.01

Table S6 – Extended models: Estimating temporal trends in internal migration

<u>Outcome: Annual out-migration flows</u>	
(1)	
Reference: 1960-1969 period	
1970-1979 period	-0.0310 (0.0508)
1980-1989 period	0.2682*** (0.0598)
1990-1999 period	0.5831*** (0.0649)
2000-2009 period	0.5501*** (0.0562)
2010-2019 period	0.7787*** (0.0707)
.....	
Origin population	-5.47e-9 (5.84e-9)
Log(distance)	-0.8145*** (0.0297)
Adjacent regions	0.5806*** (0.0473)
Time interval (5 years)	-0.3633*** (0.0475)
Origin FE	Yes
Destination FE	Yes
SE: Clustered	by: origin
Observations	107,916
Pseudo R2	0.87416
BIC	47,281,808.20

Note: PPML fixed effects gravity models. Poisson regression coefficients with cluster robust standard errors in parentheses. Clustering of standard errors at the origin region level. The outcome variable is the total annual migration flows from origin to destination regions. P-values: * 0.1 ** 0.05 *** 0.01

Table S7 – Extended analyses: Modeling non-linear drought and aridity impacts

	Outcome: Annual out-migration rate				
	(1)	(2)	(3)	(4)	(5)
AI		0.0684*** (0.0206)			
AI ²		0.0152 (0.0103)			
PDSI			0.0493*** (0.0152)		
PDSI ²			0.0225** (0.0095)		
SPEI03				0.0639*** (0.0190)	
SPEI03 ²				0.0356*** (0.0118)	
SPEI12					0.0579*** (0.0185)
SPEI12 ²					0.0221** (0.0107)
Log(distance)	-0.7632*** (0.0407)	-0.7636*** (0.0407)	-0.7635*** (0.0407)	-0.7635*** (0.0408)	-0.7635*** (0.0407)
Adjacent regions	0.6325*** (0.0861)	0.6324*** (0.0862)	0.6324*** (0.0861)	0.6325*** (0.0862)	0.6325*** (0.0861)
Time interval (5 years)	-0.1639 (0.1246)	-0.1461 (0.1293)	-0.1411 (0.1272)	-0.1273 (0.1260)	-0.1292 (0.1295)
Worldregion x decade FE.	Yes	Yes	Yes	Yes	Yes
Origin FE	Yes	Yes	Yes	Yes	Yes
Destination FE	Yes	Yes	Yes	Yes	Yes
SE: Clustered	by: origin	by: origin	by: origin	by: origin	by: origin
Observations	107,916	107,916	107,916	107,916	107,916
Pseudo R2	0.22845	0.22859	0.22855	0.22865	0.22857
BIC	34,224.90	34,247.90	34,247.90	34,247.80	34,247.90

Note: PPML fixed effects gravity models. Poisson regression coefficients with cluster robust standard errors in parentheses. Clustering of standard errors at the origin region level. Input variables: Aridity Index (AI), Palmer Drought Severity Index (PDSI), Standardized Precipitation Evapotranspiration Index (SPEI). The outcome variable is the annual out-migration rate. P-values: * 0.1 ** 0.05 *** 0.01

Table S8 – Extended models: Estimating migration impacts for different world regions

	Outcome: Annual out-migration rate			
	(1)	(2)	(3)	(4)
AI	-0.0866*** (0.0243)			
AI x EastAsia&Pacific	0.0679** (0.0311)			
AI x MiddleEast&NorthAfrica	0.3885 (0.2727)			
AI x NorthAmerica	0.0907*** (0.0274)			
AI x NortheasternEurope&CentralAsia	0.0995*** (0.0260)			
AI x SouthAmerica	0.2006*** (0.0532)			
AI x SouthAsia	0.5054*** (0.1065)			
AI x SouthernEurope	0.6732*** (0.1236)			
AI x Sub-SaharanAfrica	0.1287*** (0.0311)			
PDSI		-0.0737*** (0.0209)		
PDSI x EastAsia&Pacific		0.0586** (0.0262)		
PDSI x MiddleEast&NorthAfrica		0.1778 (0.1986)		
PDSI x NorthAmerica		0.0616** (0.0255)		
PDSI x Northeastern Europe&CentralAsia		0.0583** (0.0231)		
PDSI x SouthAmerica		0.1160** (0.0467)		
PDSI x SouthAsia		0.3320*** (0.0933)		
PDSI x SouthernEurope		0.7367*** (0.1268)		
PDSI x Sub-SaharanAfrica		0.1002*** (0.0264)		
SPEI03			-0.0928*** (0.0257)	
SPEI03 x EastAsia&Pacific			0.0761** (0.0336)	
SPEI03 x MiddleEast&NorthAfrica			0.1939 (0.2067)	
SPEI03 x NorthAmerica			0.0940*** (0.0283)	
SPEI03 x Northeastern Europe&CentralAsia			0.0732*** (0.0244)	
SPEI03 x SouthAmerica			0.1618*** (0.0560)	
SPEI03 x SouthAsia			0.4112*** (0.1207)	
SPEI03 x SouthernEurope			0.5762*** (0.1188)	
SPEI03 x Sub-SaharanAfrica			0.1380*** (0.0396)	
SPEI12				-0.0824*** (0.0242)
SPEI12 x EastAsia&Pacific				0.0975*** (0.0301)
SPEI12 x MiddleEast&NorthAfrica				0.3450 (0.2366)
SPEI12 x NorthAmerica				0.0891*** (0.0277)
SPEI12 x Northeastern Europe&CentralAsia				0.0823*** (0.0245)

SPEI12 x SouthAmerica				0.1594*** (0.0531)
SPEI12 x SouthAsia				0.4484*** (0.1192)
SPEI12 x SouthernEurope				0.7002*** (0.1340)
SPEI12 x Sub-SaharanAfrica				0.1180*** (0.0333)
AI in destination	-0.0298 (0.0210)			
PDSI in destination		0.0083 (0.0174)		
SPEI03 in destination			-0.0033 (0.0208)	
SPEI12 in destination				-0.0152 (0.0193)
Log(distance)	-0.7638*** (0.0407)	-0.7645*** (0.0406)	-0.7636*** (0.0408)	-0.7637*** (0.0407)
Adjacent regions	0.6334*** (0.0861)	0.6324*** (0.0860)	0.6329*** (0.0862)	0.6330*** (0.0861)
Time interval (5 years)	0.0764 (0.1416)	0.0903 (0.1389)	0.0933 (0.1532)	0.1824 (0.1667)
Worldregion x decade FE	Yes	Yes	Yes	Yes
Origin FE	Yes	Yes	Yes	Yes
Destination FE	Yes	Yes	Yes	Yes
Destination climate controlled	Yes	Yes	Yes	Yes
SE: Clustered	by: origin	by: origin	by: origin	by: origin
Observations	107,841	107,446	107,841	107,841
Squared Cor.	0.22944	0.22923	0.22927	0.22931
Pseudo R2	34,267.80	34,071.10	34,268.00	34,267.90
BIC	107,841	107,446	107,841	107,841

Note: PPML fixed effects, gravity models. Poisson regression coefficients with cluster robust standard errors in parentheses. Clustering of standard errors at the origin region level. Input variables: Aridity Index (AI), Palmer Drought Severity Index (PDSI), Standardized Precipitation Evapotranspiration Index (SPEI). The outcome variable is the annual out-migration rate. P-values: * 0.1 ** 0.05 *** 0.01

Table S9 – Extended models: Estimating migration impacts by world regions and ecological zones

	Outcome: Annual out-migration rate			
	(1) AI	(2) PDSI	(3) SPEI03	(4) SPEI12
Climate	-1.315** (0.5340)	-0.0974*** (0.0277)	-0.3995*** (0.1330)	-0.2344*** (0.0756)
Climate x EastAsia & Pacific	1.495*** (0.4947)	0.0994*** (0.0317)	0.4646*** (0.1524)	0.3378*** (0.0883)
Climate x MiddleEast & NorthAfrica	-5.659 (16.54)	0.1536 (0.2771)	0.4152 (0.4881)	0.5611 (0.3537)
Climate x North America	1.297** (0.5698)	0.0786** (0.0331)	0.3932*** (0.1432)	0.2551*** (0.0834)
Climate x Northeastern Europe & Central Asia	1.485*** (0.5598)	0.0899*** (0.0335)	0.2282* (0.1329)	0.2418*** (0.0830)
Climate x South America	2.021*** (0.6302)	0.1429*** (0.0502)	0.5928*** (0.1907)	0.4319*** (0.1311)
Climate x South Asia	7.460*** (1.614)	0.3908*** (0.1302)	2.031*** (0.5930)	1.253*** (0.3324)
Climate x Southern Europe	9.775*** (1.688)	0.7904*** (0.1525)	2.545*** (0.5894)	1.631*** (0.3564)
Climate x Sub-Saharan Africa	1.312** (0.6010)	0.1178*** (0.0405)	0.5348*** (0.1704)	0.3034*** (0.0995)
Climate x Hyper-arid/arid	3.739** (1.799)	0.0649** (0.0298)	0.2484 (0.1795)	0.1106 (0.1070)
Climate x Sub-humid/Semi-arid	0.8883 (0.5432)	0.0069 (0.0401)	0.1498 (0.1318)	0.0290 (0.0737)
Climate destination	0.2076 (0.4411)	-0.0083 (0.0278)	0.0344 (0.1042)	0.0622 (0.0585)
Log(distance)	-0.7644*** (0.0406)	-0.7646*** (0.0406)	-0.7637*** (0.0408)	-0.7639*** (0.0407)
Adjacent regions	0.6327*** (0.0861)	0.6320*** (0.0860)	0.6325*** (0.0862)	0.6324*** (0.0861)
Time interval (5 years)	-0.0553 (0.1233)	0.0999 (0.1480)	0.1000 (0.1617)	0.1953 (0.1857)
Worldregion x decade FE	Yes	Yes	Yes	Yes
Origin FE	Yes	Yes	Yes	Yes
Destination FE	Yes	Yes	Yes	Yes
Destination climate controlled	Yes	Yes	Yes	Yes
SE: Clustered	by: origin	by: origin	by: origin	by: origin
Observations	107,916	107,916	107,916	107,916
Squared Cor.	0.71159	0.7161	0.70317	0.70705
Pseudo R2	0.20294	0.20277	0.20277	0.20269
BIC	34,369.20	34,369.40	34,369.40	34,369.50

Note: PPML fixed effects, gravity models. Poisson regression coefficients with cluster robust standard errors in parentheses. Clustering of standard errors at the origin region level. Input variables: Aridity Index (AI), Palmer Drought Severity Index (PDSI), Standardized Precipitation Evapotranspiration Index (SPEI). The outcome variable is the annual out-migration rate. P-values: * 0.1 ** 0.05 *** 0.01

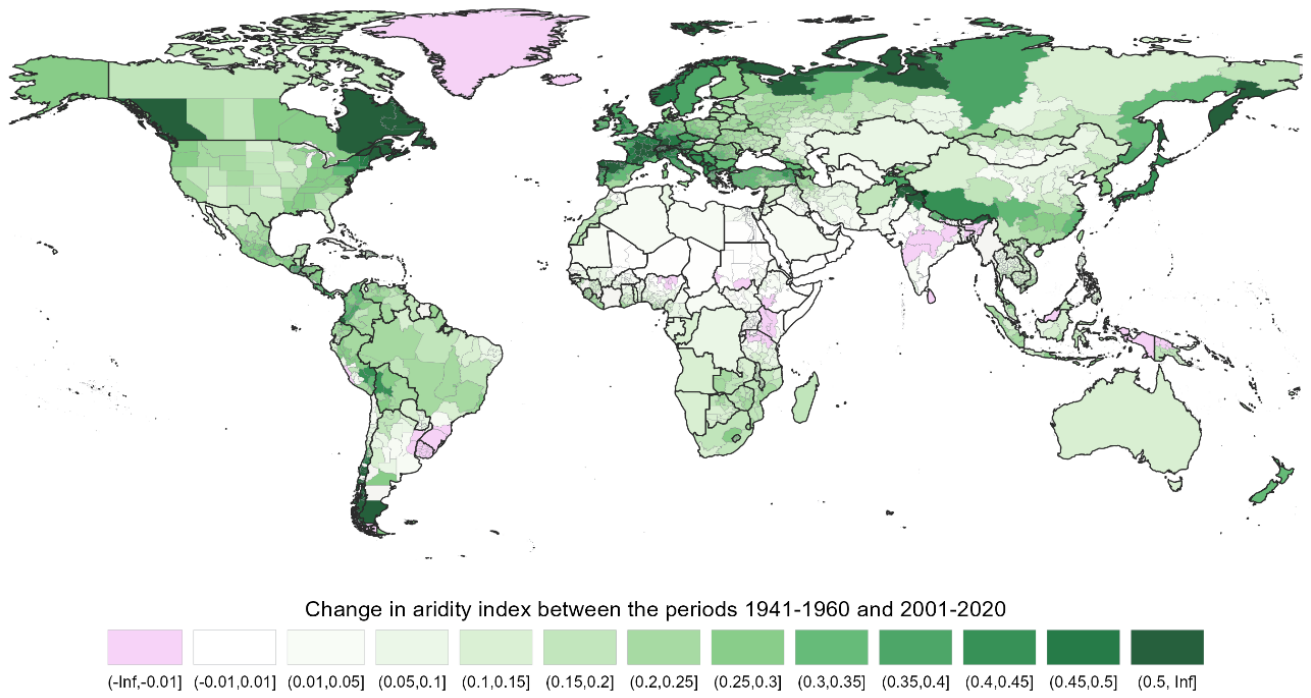


Figure S5. Projected changes in the Aridity Index under a 4°C warming scenario (RCP8.5). The scaling was changed so that positive values reflect higher dryness. Projection data were obtained from Wang et al. (2021).

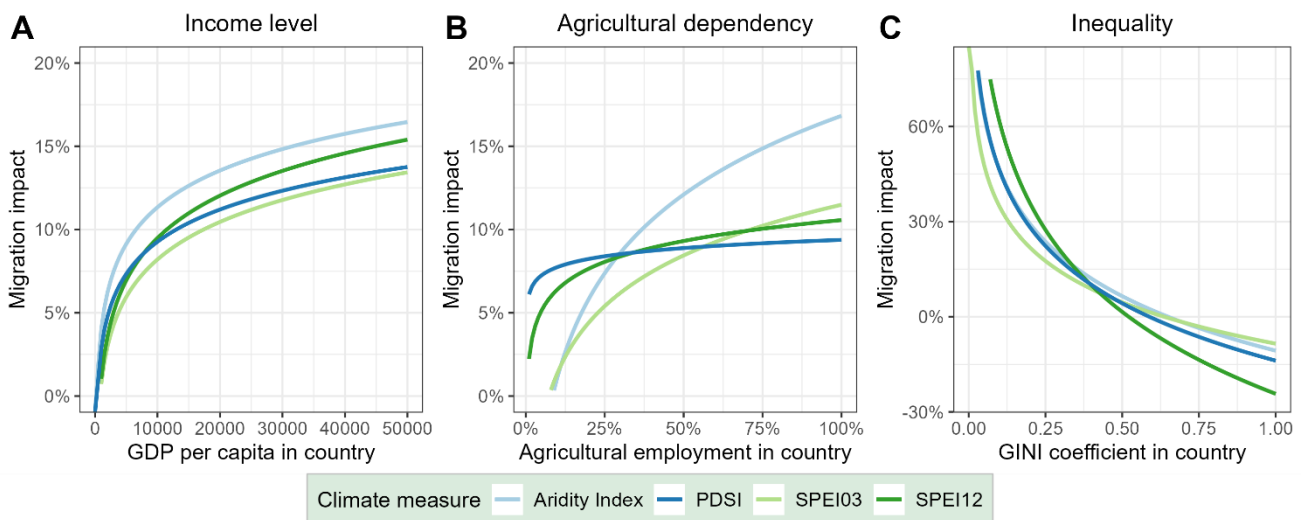


Figure S6. The role of country background characteristics in shaping migration responses to drought and aridity.

Panel A shows interactions in environmental effects on migration by GDP per capita at the country level. Panel B shows interactions by the agricultural employment share in the country. Panel C shows interactions by the level of inequality in the country as measured with the GINI coefficient. The y-axes show the marginal effects of a one standard deviation change in the climate indicators on the out-migration rate. Increasing (decreasing) functions indicate increasing (decreasing) migration impacts with higher levels of the interaction variable. All models estimating interactions with agricultural employment and the GINI coefficient also control for interactions with GDP per capita to rule out confounding wealth effects.

Table S10 – Extended analyses: Interactions with GDP per capita at the regional level

	Outcome: Annual out-migration rate			
	(1)	(2)	(3)	(4)
AI	-0.04477			
AI x log(GDP pc)	0.0384** (0.0174)			
PDSI		-0.03973		
PDSI x log(GDP pc)		0.0340** (0.0166)		
SPEI03			-0.3538** (0.1630)	
SPEI03 x log(GDP pc)			0.0444** (0.0181)	
SPEI12				-0.0454
SPEI12x log(GDP pc)				0.0381** (0.0173)
Log(GDP pc)	0.0319 (0.0903)	0.0576 (0.0913)	0.0248 (0.0914)	0.0403 (0.0909)
Log(distance)	-0.7565*** (0.0468)	-0.7573*** (0.0469)	-0.7567*** (0.0468)	-0.7566*** (0.0468)
Adjacent regions	0.6350*** (0.0980)	0.6344*** (0.0981)	0.6347*** (0.0980)	0.6348*** (0.0980)
Time interval (5 years)	-0.8963*** (0.1570)	-0.8612*** (0.1487)	-0.8596*** (0.1526)	-0.8708*** (0.1581)
Destination climate controlled	Yes	Yes	Yes	Yes
Worldregion x decade FE.	Yes	Yes	Yes	Yes
Origin FE	Yes	Yes	Yes	Yes
Destination FE	Yes	Yes	Yes	Yes
Destination climate controlled	Yes	Yes	Yes	Yes
SE: Clustered	by: origin	by: origin	by: origin	by: origin
Observations	77,226	76,890	77,226	77,226
Pseudo R2	0.21437	0.21421	0.21444	0.21433
BIC	31,811.90	31,619.10	31,811.80	31,811.90

Note: PPML fixed effects, gravity models. Poisson regression coefficients with cluster robust standard errors in parentheses. Clustering of standard errors at the origin region level. Input variables: Aridity Index (AI), Palmer Drought Severity Index (PDSI), Standardized Precipitation Evapotranspiration Index (SPEI). The outcome variable is the annual out-migration rate. P-values: * 0.1 ** 0.05 *** 0.01

Table S11 – Extended analyses: Interactions with GDP per capita and agricultural employment at the regional level

	Outcome: Annual out-migration rate			
	(1)	(2)	(3)	(4)
AI	-0.6883*** (0.2462)			
AI x log(GDP pc)	0.0973*** (0.0312)			
AI x log(% agr. employment)	0.0622*** (0.0205)			
PDSI		-0.5449** (0.2185)		
PDSI x log(GDP pc)		0.0766*** (0.0271)		
PDSI x log(% agr. employment)		0.0489*** (0.0181)		
SPEI03			-0.8357*** (0.2872)	
SPEI03 x log(GDP pc)			0.1147*** (0.0376)	
SPEI03 x log(% agr. employment)			0.0743*** (0.0287)	
SPEI12				-0.7310*** (0.2629)
SPEI12x log(GDP pc)				0.1047*** (0.0343)
SPEI12x log(% agr. employment)				0.0755*** (0.0253)
Log(GDP pc)	-0.0641 (0.1049)	-0.0317 (0.1062)	-0.0754 (0.1009)	-0.0482 (0.1032)
Log(% agr. employment)	-0.2507 (0.1524)	-0.2546 (0.1554)	-0.2755* (0.1447)	-0.2491 (0.1522)
Log(distance)	-0.7533*** (0.0505)	-0.7540*** (0.0506)	-0.7539*** (0.0506)	-0.7534*** (0.0505)
Adjacent regions	0.6349*** (0.1044)	0.6345*** (0.1045)	0.6345*** (0.1044)	0.6346*** (0.1044)
Time interval (5 years)	-0.2443** (0.1238)	-0.2513** (0.1229)	-0.2410** (0.1213)	-0.2062* (0.1215)
Destination climate controlled	Yes	Yes	Yes	Yes
Worldregion x decade FE.	Yes	Yes	Yes	Yes
Origin FE	Yes	Yes	Yes	Yes
Destination FE	Yes	Yes	Yes	Yes
Destination climate controlled	Yes	Yes	Yes	Yes
SE: Clustered	by: origin	by: origin	by: origin	by: origin
Observations	68182	68182	68182	68182
Pseudo R2	0.21722	0.21705	0.21729	0.21719
BIC	27848.6	27848.7	27848.6	27848.6

Note: PPML fixed effects, gravity models. Poisson regression coefficients with cluster robust standard errors in parentheses. Clustering of standard errors at the origin region level. Input variables: Aridity Index (AI), Palmer Drought Severity Index (PDSI), Standardized Precipitation Evapotranspiration Index (SPEI). The outcome variable is the annual out-migration rate. P-values: * 0.1 ** 0.05 *** 0.01

Table S12 – Extended analyses: Interactions with GDP per capita and urban population share

	Outcome: Annual out-migration rate			
	(1)	(2)	(3)	(4)
AI	-1.821*** (0.6192)			
AI x log(GDP pc)	0.2035*** (0.0697)			
AI x log(% urban pop)	-0.1163** (0.0549)			
PDSI		-2.028*** (0.6881)		
PDSI x log(GDP pc)		0.2271*** (0.0779)		
PDSI x log(% urban pop)		-0.1349** (0.0639)		
SPEI03			-1.925*** (0.6752)	
SPEI03 x log(GDP pc)			0.2142*** (0.0775)	
SPEI03 x log(% urban pop)			-0.1108** (0.0483)	
SPEI12				0.2204*** (0.0773)
SPEI12x log(GDP pc)				-1.960*** (0.6799)
SPEI12x log(% urban pop)				-0.1122** (0.0550)
Log(GDP pc)	-0.0961 (0.1115)	-0.1288 (0.1161)	-0.1233 (0.1169)	-0.1157 (0.1146)
Log(% urban pop)	0.1375 (0.1928)	0.1549 (0.1913)	0.1440 (0.1907)	0.1352 (0.1913)
Log(distance)	-0.8262*** (0.0737)	-0.8277*** (0.0739)	-0.8265*** (0.0736)	-0.8261*** (0.0738)
Adjacent regions	0.6246*** (0.1483)	0.6236*** (0.1483)	0.6245*** (0.1482)	0.6248*** (0.1483)
Time interval (5 years)	-1.092*** (0.2384)	-1.143*** (0.2335)	-1.225*** (0.2303)	-1.105*** (0.2359)
Destination climate controlled	Yes	Yes	Yes	Yes
Worldregion x decade FE.	Yes	Yes	Yes	Yes
Origin FE	Yes	Yes	Yes	Yes
Destination FE	Yes	Yes	Yes	Yes
Destination climate controlled	Yes	Yes	Yes	Yes
SE: Clustered	by: origin	by: origin	by: origin	by: origin
Observations	50340	50015	50340	50340
Pseudo R2	0.24541	0.24542	0.24538	0.24543
BIC	26558	26379.4	26558	26558

Note: PPML fixed effects, gravity models. Poisson regression coefficients with cluster robust standard errors in parentheses. Clustering of standard errors at the origin region level. Input variables: Aridity Index (AI), Palmer Drought Severity Index (PDSI), Standardized Precipitation Evapotranspiration Index (SPEI). The outcome variable is the annual out-migration rate. P-values: * 0.1 ** 0.05 *** 0.01

Table S13 – Extended analyses: Interactions with standardized GDP per capita

	Outcome: Annual out-migration rate			
	(1)	(2)	(3)	(4)
AI	-0.0334** (0.0134)			
AI x stand. GDP pc origin	0.0025 (0.0157)			
AI x stand. GDP pc destination	0.0774*** (0.0218)			
PDSI		-0.0277** (0.0128)		
PDSI x stand. GDP pc origin		-0.0214 (0.0202)		
PDSI x stand. GDP pc destination		0.0620*** (0.0225)		
SPEI03			-0.0330** (0.0153)	
SPEI03 x stand. GDP pc origin			0.0416*** (0.0113)	
SPEI03 x stand. GDP pc destination			0.0606** (0.0237)	
SPEI12				0.0213** (0.0107)
SPEI12 x stand. GDP pc origin				-0.0284** (0.0131)
SPEI12 x stand. GDP pc destination				0.0647*** (0.0236)
stand. GDP pc origin	-0.0284 (0.0440)	-0.0301 (0.0464)	-0.0301 (0.0444)	-0.0303 (0.0448)
stand. GDP pc destination	-0.0565 (0.0402)	-0.0401 (0.0359)	-0.0777* (0.0465)	-0.0723* (0.0425)
Log(distance)	-0.7571*** (0.0467)	-0.7566*** (0.0468)	-0.7592*** (0.0468)	-0.7584*** (0.0468)
Adjacent regions	0.6345*** (0.0980)	0.6343*** (0.0980)	0.6339*** (0.0979)	0.6340*** (0.0980)
Time interval (5 years)	-0.9380*** (0.1599)	-0.8785*** (0.1485)	-0.8792*** (0.1517)	-0.9112*** (0.1588)
Destination climate controlled	Yes	Yes	Yes	Yes
Worldregion x decade FE.	Yes	Yes	Yes	Yes
Origin FE	Yes	Yes	Yes	Yes
Destination FE	Yes	Yes	Yes	Yes
Destination climate controlled	Yes	Yes	Yes	Yes
SE: Clustered	by: origin	by: origin	by: origin	by: origin
Observations	77202	76866	77202	77202
Pseudo R2	0.21439	0.21425	0.21452	0.21436
BIC	31822.2	31629.4	31822.1	31822.2

Note: PPML fixed effects, gravity models. Poisson regression coefficients with cluster robust standard errors in parentheses. Clustering of standard errors at the origin region level. Input variables: Aridity Index (AI), Palmer Drought Severity Index (PDSI), Standardized Precipitation Evapotranspiration Index (SPEI). The outcome variable is the annual out-migration rate. P-values: * 0.1 ** 0.05 *** 0.01

Table S14 – Extended analyses: Interactions with standardized agricultural employment

	Outcome: Annual out-migration rate			
	(1)	(2)	(3)	(4)
AI	0.0791*** (0.0229)			
AI x stand. agr. employment origin	-0.0014 (0.0064)			
AI x stand. agr. employment destination	0.0263 (0.0168)			
PDSI		0.0554*** (0.0183)		
PDSI x stand. agr. employment origin		0.0147* (0.0082)		
PDSI x stand. agr. employment destination		0.0152 (0.0129)		
SPEI03			0.0693*** (0.0212)	
SPEI03 x stand. agr. employment origin			-0.0004 (0.0073)	
SPEI03 x stand. agr. employment destination			0.0575** (0.0248)	
SPEI12				0.0014 (0.0068)
SPEI12 x stand. agr. employment origin				0.0647*** (0.0207)
SPEI12 x stand. agr. employment destination				0.0402** (0.0186)
stand. agr. employment origin	-0.1101 (0.1295)	-0.1156 (0.1335)	-0.1210 (0.1279)	-0.1176 (0.1304)
stand. agr. employment destination	-0.0300 (0.0643)	-0.0270 (0.0632)	-0.0260 (0.0644)	-0.0270 (0.0641)
Log(distance)	-0.7627*** (0.0432)	-0.7627*** (0.0432)	-0.7626*** (0.0432)	-0.7625*** (0.0433)
Adjacent regions	0.6339*** (0.0923)	0.6337*** (0.0923)	0.6335*** (0.0922)	0.6338*** (0.0923)
Time interval (5 years)	0.0902 (0.1646)	0.0895 (0.1661)	0.1425 (0.1635)	0.1110 (0.1668)
Destination climate controlled	Yes	Yes	Yes	Yes
Worldregion x decade FE.	Yes	Yes	Yes	Yes
Origin FE	Yes	Yes	Yes	Yes
Destination FE	Yes	Yes	Yes	Yes
Destination climate controlled	Yes	Yes	Yes	Yes
SE: Clustered	by: origin	by: origin	by: origin	by: origin
Observations	97814	97445	97814	97814
Pseudo R2	0.21281	0.21267	0.21295	0.2128
BIC	30388.4	30205.5	30388.2	30388.4

Note: PPML fixed effects, gravity models. Poisson regression coefficients with cluster robust standard errors in parentheses. Clustering of standard errors at the origin region level. Input variables: Aridity Index (AI), Palmer Drought Severity Index (PDSI), Standardized Precipitation Evapotranspiration Index (SPEI). The outcome variable is the annual out-migration rate. P-values: * 0.1 ** 0.05 *** 0.01

Table S15 – Extended analyses: Interactions with standardized urban population share

	Outcome: Annual out-migration rate			
	(1)	(2)	(3)	(4)
AI	0.0562*			
	(0.0313)			
AI x stand. urban pop. origin	0.0368***			
	(0.0104)			
AI x stand. urban pop. destination	-0.00048			
PDSI		0.0619*		
		(0.0338)		
PDSI x stand. urban pop. origin		-0.0001		
		(0.0119)		
PDSI x stand. urban pop. destination		-0.00056		
SPEI03			0.0154	
			(0.0304)	
SPEI03 x stand. urban pop. origin			0.0587***	
			(0.0168)	
SPEI03 x stand. urban pop. destination			-0.0201	
			(0.0190)	
SPEI12				0.0377***
				(0.0104)
SPEI12 x stand. urban pop. origin				0.0431
				(0.0312)
SPEI12 x stand. urban pop. destination				-0.00044
stand. urban pop. origin	0.3920***	0.4057***	0.3971***	0.3965***
	(0.1160)	(0.1215)	(0.1201)	(0.1188)
stand. urban pop. destination	0.2399***	0.2265***	0.2430***	0.2334***
	(0.0528)	(0.0508)	(0.0528)	(0.0514)
Log(distance)	-0.8115***	-0.8106***	-0.8150***	-0.8130***
	(0.0610)	(0.0615)	(0.0609)	(0.0613)
Adjacent regions	0.6340***	0.6356***	0.6304***	0.6327***
	(0.1278)	(0.1284)	(0.1276)	(0.1281)
Time interval (5 years)	-1.223***	-1.207***	-1.234***	-1.216***
	(0.1085)	(0.1110)	(0.1078)	(0.1078)
Destination climate controlled	Yes	Yes	Yes	Yes
Worldregion x decade FE.	Yes	Yes	Yes	Yes
Origin FE	Yes	Yes	Yes	Yes
Destination FE	Yes	Yes	Yes	Yes
Destination climate controlled	Yes	Yes	Yes	Yes
SE: Clustered	by: origin	by: origin	by: origin	by: origin
Observations	70830	70446	70830	70830
Pseudo R2	0.26401	0.26382	0.26407	0.26397
BIC	29226.4	29044.3	29226.3	29226.4

Note: PPML fixed effects, gravity models. Poisson regression coefficients with cluster robust standard errors in parentheses. Clustering of standard errors at the origin region level. Input variables: Aridity Index (AI), Palmer Drought Severity Index (PDSI), Standardized Precipitation Evapotranspiration Index (SPEI). The outcome variable is the annual out-migration rate. P-values: * 0.1 ** 0.05 *** 0.01

Table S15 – Robustness test: Models controlling for lead values of climate indicators

	Outcome: Annual out-migration rate				
	(1)	(2)	(3)	(4)	(5)
AI		0.0873*** (0.0216)			
AI lead		0.0284 (0.0222)			
PDSI			0.0642*** (0.0167)		
PDSI lead			0.0122 (0.0190)		
SPEI03				0.0895*** (0.0231)	
SPEI03 lead				0.0247 (0.0188)	
SPEI12					0.0806*** (0.0209)
SPEI12 lead					0.0036 (0.0179)
Log(distance)	-0.7632*** (0.0410)	-0.7573*** (0.0430)	-0.7572*** (0.0430)	-0.7573*** (0.0431)	-0.7573*** (0.0430)
Adjacent regions	0.6334*** (0.0865)	0.6337*** (0.0907)	0.6335*** (0.0906)	0.6336*** (0.0907)	0.6336*** (0.0906)
Time interval (5 years)	-0.4242*** (0.1255)	-0.0122 (0.1218)	0.0024 (0.1298)	0.0052 (0.1258)	0.0387 (0.1314)
Worldregion x decade FE.	Yes	Yes	Yes	Yes	Yes
Origin FE	Yes	Yes	Yes	Yes	Yes
Destination FE	Yes	Yes	Yes	Yes	Yes
SE: Clustered	by: origin	by: origin	by: origin	by: origin	by: origin
Observations	107,916	100,371	100,371	100,371	100,371
Pseudo R2	0.23097	0.23524	0.23514	0.23522	0.23518
BIC	35,079.70	32,476.50	32,476.60	32,476.60	32,476.60

Note: PPML fixed effects, gravity models. Poisson regression coefficients with cluster robust standard errors in parentheses. Clustering of standard errors at the origin region level. Input variables: Aridity Index (AI), Palmer Drought Severity Index (PDSI), Standardized Precipitation Evapotranspiration Index (SPEI). The outcome variable is the annual out-migration rate. P-values: * 0.1 ** 0.05 *** 0.01

Table S16 – Robustness test: Models controlling for destination region climate

	Outcome: Annual out-migration rate				
	(1)	(2)	(3)	(4)	(5)
AI origin		0.0778*** (0.0279)			
AI destination		-0.0200 (0.0217)			
PDSI origin			0.0463** (0.0201)		
PDSI destination			0.0052 (0.0168)		
SPEI03 origin				0.0619** (0.0270)	
SPEI03 destination				0.0173 (0.0200)	
SPEI12 origin					0.0638** (0.0250)
SPEI12 destination					-0.0092 (0.0187)
Log(distance)	-0.7632*** (0.0407)	-0.7637*** (0.0407)	-0.7639*** (0.0408)	-0.7634*** (0.0407)	-0.7635*** (0.0407)
Adjacent regions	0.6325*** (0.0861)	0.6327*** (0.0862)	0.6323*** (0.0862)	0.6326*** (0.0862)	0.6327*** (0.0862)
Time interval (5 years)	-0.1639 (0.1246)	-0.1624 (0.1263)	-0.1522 (0.1257)	-0.1281 (0.1280)	-0.1391 (0.1295)
Worldregion x decade FE.	Yes	Yes	Yes	Yes	Yes
Origin FE	Yes	Yes	Yes	Yes	Yes
Destination FE	Yes	Yes	Yes	Yes	Yes
SE: Clustered	by: origin	by: origin	by: origin	by: origin	by: origin
Observations	107,916	107,841	107,446	107,841	107,841
Pseudo R2	0.22845	0.22863	0.22852	0.22863	0.22859
BIC	34,224.90	34,176.00	33,979.30	34,176.00	34,176.00

Note: PPML fixed effects, gravity models. Poisson regression coefficients with cluster robust standard errors in parentheses. Clustering of standard errors at the origin region level. Input variables: Aridity Index (AI), Palmer Drought Severity Index (PDSI), Standardized Precipitation Evapotranspiration Index (SPEI). The outcome variable is the annual out-migration rate. P-values: * 0.1 ** 0.05 *** 0.01